Synthesis and Properties of Substituted CBI Analogs of CC-1065 and the Duocarmycins Incorporating the 7-Methoxy-1,2,9,9a-tetrahydrocyclopropa[*c*]benz[*e*]indol-4-one (MCBI) Alkylation Subunit: Magnitude of Electronic Effects on the Functional Reactivity

Dale L. Boger,* Jeffrey A. McKie, Hui Cai, Barbara Cacciari, and P. G. Baraldi[1]

Department of Chemistry, The Scripps Research Institute, 10666 North Torrey Pines Road, La Jolla, California 92037

Received November 16, 1995[⊗]

The synthesis of 7-methoxy-1,2,9,9a-tetrahydrocyclopropa[*c*]benz[*e*]indol-4-one (MCBI), a substituted CBI derivative bearing a C7 methoxy group para to the C4 carbonyl, is described in efforts that establish the magnitude of potential electronic effects on the chemical and functional reactivity of the agents. The core structure of the MCBI alkylation subunit was prepared by a modified Stobbe condensation/Friedel−Crafts acylation for generation of the appropriately functionalized naphthalene precursors (**15** and **20**) followed by 5-*exo-trig* aryl radical−alkene cyclization (**24** → **25**, **32** → **33**) for completion of the synthesis of the 1,2-dihydro-3*H*-benz[*e*]indole skeleton and final Ar-3′ alkylation of **28** for introduction of the activated cyclopropane. Two approaches to the implementation of the key 5-*exo-trig* free radical cyclization are detailed with the former proceeding with closure of **24** to provide **25** in which the required product functionalization was introduced prior to cyclization and the latter with Tempo trap of the cyclization product of the unfunctionalized alkene substrate **32** to provide **33**. The latter concise approach provided the MCBI subunit and its immediate precursor in 12−13 steps in superb overall conversions (27−30%). Resolution of an immediate MCBI precursor and its incorporation into both enantiomers of **39**−**46**, analogs of CC-1065 and the duocarmycins, are detailed. A study of the solvolysis reactivity and regioselectivity of *N*-BOC-MCBI (**29**) revealed that introduction of the C7 methoxy group accelerates the rate of solvolysis by only 1.2−1.06×. This remarkably modest effect is inconsistent with C4 carbonyl protonation as the slow and rate-determining step of solvolysis or acid-catalyzed nucleophilic addition but is consistent with a mechanism in which protonation is rapid and reversible followed by slow and rate-determining nucleophilic addition to the cyclopropane requiring both the presence and assistance of a nucleophile (S_N2 mechanism). No doubt this contributes to the DNA alkylation selectivity of this class of agents and suggests that the positioning of an accessible nucleophile (adenine N3) and not C4 carbonyl protonation is the rate-determining step controlling the sequence selectivity of the DNA alkylation reaction. This small electronic effect on the solvolysis rate had no impact on the solvolysis regioselectivity, and stereoelectronically-controlled nucleophilic addition to the least substituted carbon of the activated cyclopropane was observed exclusively. For the natural enantiomers, this unusually small electronic effect on functional reactivity had little or no perceptible effect on their DNA alkylation selectivity, efficiency, and relative rates or on their biological properties. Perceptible effects of the C7 methoxy substituent on the unnatural enantiomers were observed and they proved to be 4−40× more effective than the corresponding CBI-based unnatural enantiomers and comparable in cytotoxic potency with the MCBI natural enantiomers. This effect is most consistently rationalized not by a C7 methoxy substituent effect on functional reactivity but rather through introduction of additional stabilizing noncovalent interactions which increase the unnatural enantiomer DNA alkylation efficiency and further stabilize its inherently reversible DNA alkylation reaction.

(+)-CC-1065 (**1**)[2] and the duocarmycins **2** and **3**[3,4] represent the initial members of a class of exceptionally potent antitumor antibiotics that derive their biological effects through the reversible, stereoelectronically-controlled sequence-selective alkylation of DNA.[5−13] Subsequent to their disclosure, extensive efforts have been devoted to establish their DNA alkylation selectivity and its structural origin,[5−13] to establish the link between DNA alkylation and the ensuing biological properties,[14] and to define the fundamental principles underlying the relationships between structure, chemical reactivity, and biological properties.[15−40]

⊗ Abstract published in *Advance ACS Abstracts,* February 1, 1996.

(1) Dipartimento di Scienze Farmaceutiche, Universita di Ferrara, via Fossato di Mortara 17-19, I-44100 Ferrara, Italy.

(2) Hanka, L. J.; Dietz, A.; Gerpheide, S. A.; Kuentzel, S. L.; Martin, D. G. *J. Antibiot.* **1978**, *31*, 1211. Chidester, C. G.; Krueger, W. C.; Mizsak, S. A.; Duchamp, D. J.; Martin, D. G. *J. Am. Chem. Soc.* **1981**, *103*, 7629.

(3) Yasuzawa, T.; Muroi, K.; Ichimura, M.; Takahashi, I.; Ogawa, T.; Takahashi, K.; Sano, H.; Saitoh, Y. *Chem. Pharm. Bull.* **1995**, *43*, 378. Takahashi, I.; Takahashi, K.; Ichimura, M.; Morimoto, M.; Asano, K.; Kawamoto, I.; Tomita, F.; Nakano, H. *J. Antibiot.* **1988**, *41*, 1915. Yasuzawa, T.; Iida, T.; Muroi, K.; Ichimura, M.; Takahashi, K.; Sano, H. *Chem. Pharm. Bull.* **1988**, *36*, 3728. Ichimura, M.; Muroi, K.; Asano, K.; Kawamoto, I.; Tomita, F.; Morimoto, M.; Nakano, H. *J. Antibiot.* **1988**, *41*, 1285. Ohba, K.; Watabe, H.; Sasaki, T.; Takeuchi, Y.; Kodama, Y.; Nakazawa, T.; Yamamoto, H.; Shomura, T.; Sezaki, M.; Kondo, S. *J. Antibiot.* **1988**, *41*, 1515. Ishii, S.; Nagasawa, M.; Kariya, Y.; Yamamoto, H.; Inouye, S.; Kondo, S. *J. Antibiot.* **1989**, *42*, 1713.

(4) Ichimura, M.; Ogawa, T.; Takahashi, K.; Kobayashi, E.; Kawamoto, I.; Yasuzawa, T.; Takahashi, I.; Nakano, H. *J. Antibiot.* **1990**, *43*, 1037. Ichimura, M.; Ogawa, T.; Katsumata, S.; Takahashi, K.; Takahashi, I.; Nakano, H. *J. Antibiot.* **1991**, *44*, 1045.

0022-3263/96/1961-1710$12.00/0

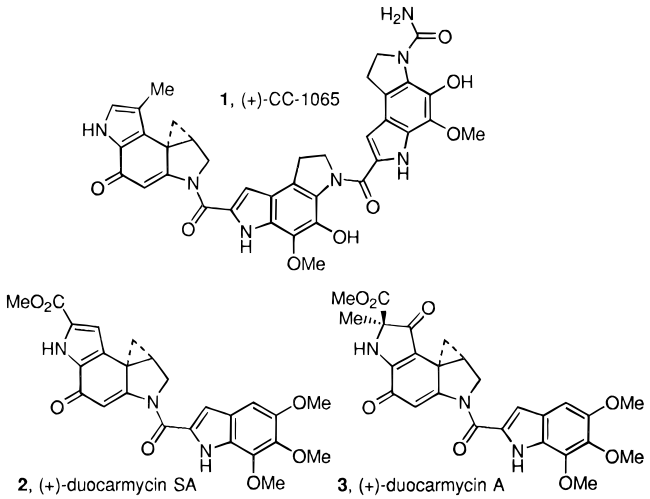

In the course of our efforts, we described the first preparation and examination of agents containing the 1,2,9,9a-tetrahydrocyclopropa[*c*]benz[*e*]indol-4-one (CBI) alkylation subunit.[24,25] Although our initial interest in this class of agents was derived from efforts to define relationships between structure, functional reactivity, and biological properties, the biological activity of the CBI-based analogs have proven especially interesting.[40] This was significant since early studies[8,12] had attributed such unique characteristics to the naturally occurring alkylation subunits that they left the perception that even small structural perturbations, let alone deep-seated structural changes, would have detrimental effects on the properties. Not only has this proven inaccurate, but the natural enantiomers of the CBI-based analogs of (+)-CC-1065 have proven chemically more stable (4×), biological more potent, and considerably more synthetically accessible[25−27] than the corresponding agents incorporating the natural CPI alkylation subunit of CC-1065.[30] Selected agents within the series exhibit not only potent cytotoxic activity but also potent and efficacious in vivo antitumor activity.[32,40]

The natural enantiomers of the CBI-based analogs have been shown to alkylate DNA with an unaltered sequence selectivity[33,34,36,37] at an enhanced rate[32−34] and with a greater efficiency than the corresponding CPI analogs,[32−34] indicating that the simplified CBI alkylation subunit offers important advantages over the natural alkylation subunit of CC-1065. In recent studies, we have presented refined models of the DNA alkylation reactions of the duocarmycins[5,6] and CC-1065[9] which accommodate the reversed and offset AT-rich adenine N3 DNA alkylation selectivity of the enantiomeric agents and their structural analogs. From this work, a beautiful explanation has emerged which explains the unusual and apparently confusing behavior of the unnatural enantiomers.[6,9,42] The diastereomeric adducts derived from the unnatural enantiomers suffer a significant destabilizing steric interaction between the CPI C7 center (CH_3) or the CBI C8 center with the base adjacent to the alkylated adenine which is not present with the natural enantiomer adducts. Consistent with this observation, the distinguishing features between the natural and unnatural enantiomers diminish or disappear as the inherent steric bulk surrounding this center is reduced or removed.[36] Because of the unnatural enantiomer sensitivity to destabilizing steric interactions surrounding the CPI C7 or CBI C8 center, the unnatural enantiomers of the CBI-based analogs are more effective than the corresponding CPI analogs displaying an even more enhanced relative

(5) Boger, D. L.; Ishizaki, T.; Zarrinmayeh, H.; Kitos, P. A.; Suntornwat, O. *J. Org. Chem.* **1990**, *55*, 4499. Boger, D. L.; Ishizaki, T.; Zarrinmayeh, H.; Munk, S. A.; Kitos, P. A.; Suntornwat, O. *J. Am. Chem. Soc.* **1990**, *112*, 8961. Boger, D. L.; Ishizaki, T.; Zarrinmayeh, H. *J. Am. Chem. Soc.* **1991**, *113*, 6645. Boger, D. L.; Yun, W. *J. Am. Chem. Soc.* **1993**, *115*, 9872. Boger, D. L.; Yun, W.; Terashima, S.; Fukuda, Y.; Nakatani, K.; Kitos, P. A.; Jin, Q. *Bioorg. Med. Chem. Lett.* **1992**, *2*, 759.

(6) Boger, D. L.; Johnson, D. S.; Yun, W. *J. Am. Chem. Soc.* **1994**, *116*, 1635.

(7) Lin, C. H.; Patel, D. J. *J. Am. Chem. Soc.* **1992**, *114*, 10658. Sugiyama, H.; Ohmori, K.; Chan, K. L.; Hosoda, M.; Asai, A.; Saito, H.; Saito, I. *Tetrahedron Lett.* **1993**, *34*, 2179. Yamamoto, K.; Sugiyama, H.; Kawanishi, S. *Biochemistry* **1993**, *32*, 1059. Asai, A.; Nagamura, S.; Saito, H. *J. Am. Chem. Soc.* **1994**, *116*, 4171.

(8) Hurley, L. H.; Reynolds, V. L.; Swenson, D. H.; Petzold, G. L.; Scahill, T. A. *Science* **1984**, *226*, 843. Reynolds, V. L.; Molineaux, I. J.; Kaplan, D. J.; Swenson, D. H.; Hurley, L. H. *Biochemistry* **1985**, *24*, 6228. Hurley, L. H.; Lee, C.-S.; McGovren, J. P.; Warpehoski, M. A.; Mitchell, M. A.; Kelly, R. C.; Aristoff, P. A. *Biochemistry* **1988**, *27*, 3886. Hurley, L. H.; Warpehoski, M. A.; Lee, C.-S.; McGovren, J. P.; Scahill, T. A.; Kelly, R. C.; Mitchell, M. A.; Wicnienski, N. A.; Gebhard, I.; Johnson, P. D.; Bradford, V. S. *J. Am. Chem. Soc.* **1990**, *112*, 4633. Warpehoski, M. A.; Harper, D. E.; Mitchell, M. A.; Monroe, T. J. *Biochemistry* **1992**, *31*, 2502.

(9) Boger, D. L.; Johnson, D. S.; Yun, W.; Tarby, C. M. *Bioorg. Med. Chem.* **1994**, *2*, 115. Boger, D. L.; Coleman, R. S.; Invergo, B. J.; Sakya, S. M.; Ishizaki, T.; Munk, S. A.; Zarrinmayeh, H.; Kitos, P. A.; Thompson, S. C. *J. Am. Chem. Soc.* **1990**, *112*, 4623.

(10) Boger, D. L.; Munk, S. A.; Zarrinmayeh, H.; Ishizaki, T.; Haught, J.; Bina, M. *Tetrahedron* **1991**, *47*, 2661.

(11) Boger, D. L. *Acc. Chem. Res.* **1995**, *28*, 20. Boger, D. L.; Johnson, D. S. *Proc. Natl. Acad. Sci. U.S.A.* **1995**, *92*, 3642. Boger, D. L. *Chemtracts: Org. Chem.* **1991**, *4*, 329. Boger, D. L. In *Proceedings of the R. A. Welch Foundation Conference on Chemical Research, XXXV. Chemistry at the Frontiers of Medicine* **1991**, *35*, 137. Boger, D. L. In *Advances in Heterocyclic Natural Products Synthesis, Vol. 2*; Pearson, W. H., Ed.; JAI Press: Greenwich, CT, 1992; pp 1−188. Boger, D. L. *Pure Appl. Chem.* **1993**, *65*, 1123. Boger, D. L. *Pure Appl. Chem.* **1994**, *66*, 837.

(12) Warpehoski, M. A. In *Advances in DNA Sequence Specific Agents*; Hurley, L. H., Ed.; JAI Press: Greenwich, CT, 1992; Vol. 1, p 217. Warpehoski, M. A. *Drugs Fut.* **1991**, *16*, 131. Warpehoski, M. A.; McGovren, J. P.; Mitchell, M. A. Hurley, L. H. In *Molecular Basis of Specificity in Nucleic Acid-Drug Interactions*; Pullman, B., Jortner, J., Eds.; Kluwer: The Netherlands, 1990; p 531. Warpehoski, M. A.; Hurley, L. H. *Chem. Res. Toxicol.* **1988**, *1*, 315. Hurley, L. H.; Draves, P. H. In *Molecular Aspects of Anticancer Drug-DNA Interactions*; Neidle, S., Waring, M., Eds.; CRC Press: Ann Arbor, MI, 1993; Vol. 1, p 89. Hurley, L. H.; Needham-VanDevanter, D. R. *Acc. Chem. Res.* **1986**, *19*, 230.

(13) Coleman, R. S.; Boger, D. L. In *Studies in Natural Product Chemistry*, Vol. 3; Rahman, A.-u.-, Ed.; Elsevier: Amsterdam, 1989; p 301. Boger, D. L. In *Heterocycles in Bioorganic Chemistry*; Bergman, J., van der Plas, H. C., Simonyl, M., Eds.; Royal Society of Chemistry: Cambridge, 1991; p 103.

(14) Boger, D. L.; Johnson, D. S.; Wrasidlo, W. *Bioorg. Med. Chem. Lett.* **1994**, *4*, 631.

(15) Wierenga, W.; Bhuyan, B. K.; Kelly, R. C.; Krueger, W. C.; Li, L. H.; McGovren, J. P.; Swenson, D. H.; Warpehoski, M. A. *Adv. Enzyme Regul.* **1986**, *25*, 141. Warpehoski, M. A.; Gebhard, I.; Kelly, R. C.; Krueger, W. C.; Li, L. H.; McGovren, J. P.; Prairie, M. D.; Wicnienski, N.; Wierenga, W. *J. Med. Chem.* **1988**, *31*, 590.

(16) Boger, D. L.; Machiya, K.; Hertzog, D. L.; Kitos, P. A.; Holmes, D. *J. Am. Chem. Soc.* **1993**, *115*, 9025. Boger, D. L.; Machiya, K. *J. Am. Chem. Soc.* **1992**, *114*, 10056. Muratake, H.; Abe, I.; Natsume, M. *Tetrahedron Lett.* **1994**, *35*, 2573.

(17) Nakatani, K.; Fukukda, Y.; Terashima, S. *Pure Appl. Chem.* **1994**, *66*, 2255. Fukuda, Y.; Itoh, Y.; Nakatani, K.; Terashima, S. *Tetrahedron* **1994**, *50*, 2793. Fukuda, Y.; Nakatani, K.; Terashima, S. *Tetrahedron* **1994**, *50*, 2809. Fukuda, Y.; Nakatani, K.; Terashima, S. *Bioorg. Med. Chem. Lett.* **1992**, *2*, 755. Fukuda, Y.; Nakatani, K.; Ito, Y.; Terashima, S. *Tetrahedron Lett.* **1990**, *31*, 6699.

(18) Wierenga, W. *J. Am. Chem. Soc.* **1981**, *103*, 5621. Magnus, P.; Gallagher, T.; Schultz, J.; Or, Y.-S.; Ananthanarayan, T. P. *J. Am. Chem. Soc.* **1987**, *109*, 2706. Kraus, G. A.; Yue, S.; Sy, J. *J. Org. Chem.* **1985**, *50*, 283. Boger, D. L.; Coleman, R. S. *J. Am. Chem. Soc.* **1988**, *110*, 1321, 4796. Boger, D. L.; Coleman, R. S. *J. Org. Chem.* **1988**, *53*, 695. Bolton, R. E.; Moody, C. J.; Pass, M.; Rees, C. W.; Tojo, G. *J. Chem. Soc., Perkin Trans. 1* **1988**, 2491. Sundberg, R. J.; Baxter, E. W.; Pitts, W. J.; Ahmed-Schofield, R.; Nishiguchi, T. *J. Org. Chem.* **1988**, *53*, 5097. Sundberg, R. J.; Pitts, W. J. *J. Org. Chem.* **1991**, *56*, 3048. Martin, V. P. *Helv. Chim. Acta* **1989**, *72*, 1554. Toyota, M.; Fukumoto, K. *J. Chem. Soc., Perkin Trans. 1* **1992**, 547. Tietze, L. F.; Grote, T. *J. Org. Chem.* **1994**, *59*, 192. Tietze, L.; Buhr, W. *Angew. Chem., Int. Ed. Engl.* **1995**, *34*, 1366.

rate and efficiency of DNA alkylation. These observations have prompted us to study the CBI-based analogs of CC-1065 and the duocarmycins in detail.

One key observation that has emerged in these studies is the direct relationship between functional stability and cytotoxic potency.[21,25] In an ongoing series of studies conducted with agents containing deep-seated modifications in the alkylation subunit which include **4**−**9**, the agents possessing the greatest solvolysis stability have been found to exhibit the most potent cytotoxic activity. Moreover, this direct relationship between functional stability and biological potency has been observed with both simple and advanced analogs of the natural products. A potential validation of this relationship was established with a series of simple N^2-substituted CBI derivatives,[35,40] where predictable linear relationships between solvolysis stability (−log *k*), cytotoxic potency (log $1/IC_{50}$, L1210), and the electron-withdrawing properties of the N^2 substituent (Hammett σ_p constant) were observed.

In efforts to verify these observations and further quantitate the magnitude of substituent electronic effects on functional reactivity, we herein report the extension of the studies to the preparation of the first substituted

4, (+)-N-BOC-CBI **5**, (+)-N-BOC-DSA **6**, (+)-N-BOC-CPI

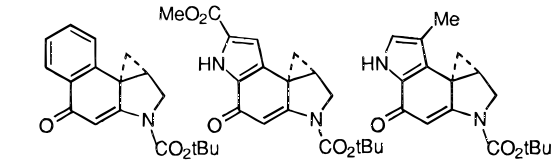

7, (+)-N-BOC-DA **8**, (+)-N-BOC-CBQ **9**, (+)-N-BOC-CI

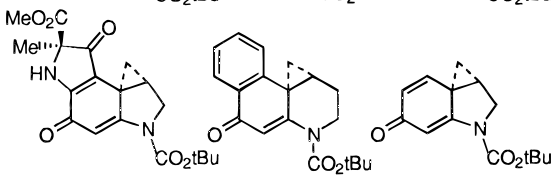

	k (s^{-1}, pH 3)	$t_{1/2}$ (pH 3)	IC_{50} (L1210)
5	1.08×10^{-6}	177 h	6 nM
4	1.45×10^{-6}	133 h	80 nM
6	5.26×10^{-6}	37 h	330 nM
7	1.75×10^{-5}	11 h	1000 nM
8	9.07×10^{-5}	2.1 h	2000 nM
9	1.98×10^{-2}	0.01 h	18000 nM

CBI derivative, 7-methoxy-1,2,9,9a-tetrahydrocyclopropa-[*c*]benz[*e*]indol-4-one (MCBI), bearing a C7 methoxy substituent para to the C4 carbonyl. The direct comparison of MCBI with CBI was anticipated to permit an assessment of the magnitude of the electronic effects of a C7 substituent on chemical reactivity and, ultimately, the relationship of this functional reactivity with the biological properties of the agents.

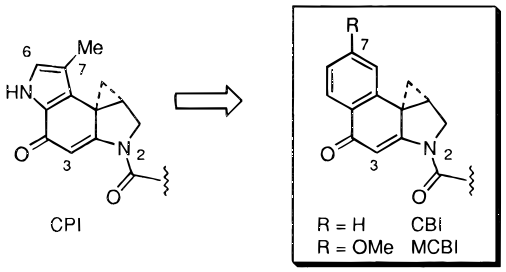

Synthesis of MCBI (30) and *N*-BOC-MCBI (29). Stobbe[43,44] condensation of 3-methoxybenzaldehyde (**10**) with diethyl succinate (3−6 equiv) effected by treatment with *t*-BuOK[44,45] (2−4 equiv, *t*-BuOH, reflux, 1−2 h, 74%) provided a 2:1 mixture of half-esters **11** which were subjected to Friedel−Crafts acylation (1.0 equiv of NaOAc, Ac_2O, reflux 5 h) to provide a mixture of **15**, its corresponding *O*-acetate **14**, and significant amounts of the isomeric Friedel−Crafts products **12**−**13** (Scheme 1). Subsequent ethanolysis (K_2CO_3, EtOH) of the resulting mixture served to hydrolyze the *O*-acetates **12** and **14**, providing a mixture of **15** and its isomer **13**, which were readily separated by chromatography. Use of this approach provided **15** in a satisfactory 40−45% overall yield from **10** without deliberate purification of the intermediates **11** or **14** but suffered from erratic conversions and the required separation of the final isomeric products. The best conversions were observed when the Friedel−Crafts acylation was conducted under moderately dilute reaction conditions (0.1 versus 0.5 M). Additional efforts

(19) CI-based analogs: Boger, D. L.; Zarrinmayeh, H.; Munk, S. A.; Kitos, P. A.; Suntornwat, O. *Proc. Natl. Acad. Sci. U.S.A.* **1991**, *88*, 1431. Boger, D. L.; Munk, S. A.; Zarrinmayeh, H. *J. Am. Chem. Soc.* **1991**, *113*, 3980. Boger, D. L.; Wysocki, R. J., Jr. *J. Org. Chem.* **1989**, *54*, 1238. Boger, D. L.; Wysocki, R. J., Jr.; Ishizaki, T. *J. Am. Chem. Soc.* **1990**, *112*, 5230. Drost, K. J.; Jones, R. J.; Cava, M. P. *J. Org. Chem.* **1989**, *54*, 5985. Tidwell, J. H.; Buchwald, S. L. *J. Org. Chem.* **1992**, *57*, 6380. Sundberg, R. J.; Baxter, E. W. *Tetrahedron Lett.* **1986**, *27*, 2687. Wang, Y.; Lown, J. W. *Heterocycles* **1993**, *36*, 1399. Wang, Y.; Gupta, R.; Huang, L.; Lown, J. W. *J. Med. Chem.* **1993**, *36*, 4172. Tietze, L. F.; Grote, T. *Chem. Ber.* **1993**, *126*, 2733. Sakamoto, T.; Kondo, Y.; Uchiyama, M.; Yamanaka, H. *J. Chem. Soc., Perkin Trans. 1* **1993**, 1941. See also refs 5 and 10.

(20) C_2BI-based analogs: Boger, D. L.; Palanki, M. S. S. *J. Am. Chem. Soc.* **1992**, *114*, 9318. Boger, D. L.; Johnson, D. S.; Palanki, M. S. S.; Kitos, P. A.; Chang, J.; Dowell, P. *Bioorg. Med. Chem.* **1993**, *1*, 27.

(21) CBQ-based analogs: Boger, D. L.; Mesini, P.; Tarby, C. M. *J. Am. Chem. Soc.* **1994**, *116*, 6461. Boger, D. L.; Mesini, P. *J. Am. Chem. Soc.* **1994**, *116*, 11335. Boger, D. L.; Mésini, P. *J. Am. Chem. Soc.* **1995**, *117*, 11647.

(22) CFI-based analogs: Mohamadi, F.; Spees, M. M.; Staten, G. S.; Marder, P.; Kipka, J. K.; Johnson, D. A.; Boger, D. L.; Zarrinmayeh, H. *J. Med. Chem.* **1994**, *37*, 232.

(23) A *p*-quinone methide analog: Boger, D. L.; Nishi, T.; Teegarden, B. R. *J. Org. Chem.* **1994**, *59*, 4943.

(24) Boger, D. L.; Ishizaki, T.; Wysocki, R. J., Jr.; Munk, S. A.; Kitos, P. A.; Suntornwat, O. *J. Am. Chem. Soc.* **1989**, *111*, 6461.

(25) Boger D. L.; Ishizaki, T.; Kitos, P. A.; Suntornwat, O. *J. Org. Chem.* **1990**, *55*, 5823.

(26) Boger, D. L.; Yun, W.; Teegarden, B. R. *J. Org. Chem.* **1992**, *57*, 2873.

(27) Boger, D. L.; McKie, J. A. *J. Org. Chem.* **1995**, *60*, 1271.

(28) Drost, K. J.; Cava, M. P. *J. Org. Chem.* **1991**, *56*, 2240.

(29) Aristoff, P. A.; Johnson, P. D. *J. Org. Chem.* **1992**, *57*, 6234.

(30) Boger, D. L.; Ishizaki, T. *Tetrahedron Lett.* **1990**, *31*, 793.

(31) Boger, D. L.; Ishizaki, T.; Zarrinmayeh, H.; Kitos, P. A.; Suntornwat, O. *Bioorg. Med. Chem. Lett.* **1991**, *1*, 55.

(32) Boger, D. L.; Ishizaki, T.; Sakya, S. M.; Munk, S. A.; Kitos, P. A.; Jin, Q.; Besterman, J. M. *Bioorg. Med. Chem. Lett.* **1991**, *1*, 115.

(33) Boger, D. L.; Munk, S. A.; Ishizaki, T. *J. Am. Chem. Soc.* **1991**, *113*, 2779.

(34) Boger, D. L.; Munk, S. A. *J. Am. Chem. Soc.* **1992**, *114*, 5487.

(35) Boger, D. L.; Yun, W. *J. Am. Chem. Soc.* **1994**, *116*, 5523.

(36) Boger, D. L.; Yun, W. *J. Am. Chem. Soc.* **1994**, *116*, 7996.

(37) Aristoff, P. A.; Johnson, P. D.; Sun, D. *J. Med. Chem.* **1993**, *36*, 1956.

(38) Boger, D. L.; Yun, W.; Johnson, D. S.; Han, N. *Bioorg. Med. Chem.* **1995**, *3*, 611.

(39) Boger, D. L.; Yun, W.; Cai, H.; Han, N. *Bioorg. Med. Chem.* **1995**, *3*, 761.

(40) Boger, D. L.; Yun, W.; Han, N. *Bioorg. Med. Chem.* **1995**, *3*, 1429.

(41) Boger, D. L.; Han, N.; Tarby, C. M.; Kitos, P. A. Unpublished studies.

(42) Boger, D. L.; Johnson, D. S. *J. Am. Chem. Soc.* **1995**, *117*, 1443.

(43) Stobbe, H. *Chem. Ber.* **1893**, *26*, 2312.

(44) Johnson, W. S.; Daub, G. H. *Org. React.* **1951**, *6*, 1.

(45) Baghos, V. B.; Nasr, F. H.; Gindy, M. *Helv. Chim. Acta* **1979**, *62*, 90.

Scheme 1

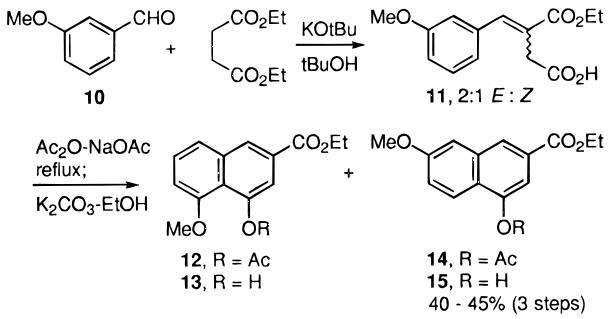

Scheme 2

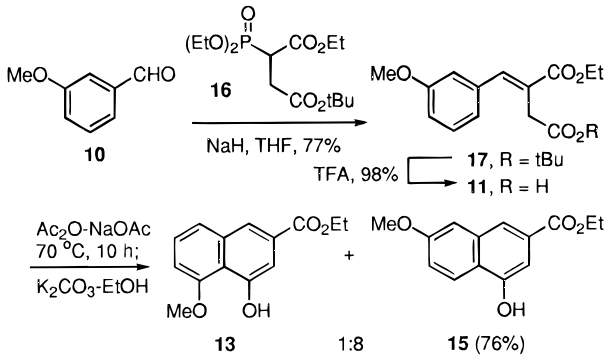

to improve this approach[46−51] failed to increase the conversions or improve the isomer ratio of **15** to **13**. In part, the 2:1 *E*:*Z* mixture of initial half esters **11** dictated a harsh set of Friedel−Crafts acylation conditions capable of isomerization and cyclization of the unproductive *Z*-isomer. Attempts to improve the ratio of isomeric products using milder reaction conditions generally afforded lower overall conversions to **15** due to the less effective cyclization of the *Z*-isomer.

This was improved significantly by conducting the Stobbe condensation in a more controlled manner. Condensation of **10** with the Wadsworth−Horner−Emmons reagent **16**[52] (1 equiv, 1.05 equiv of NaH, THF, 0 to 25 °C, 10 h, 77%) provided **17** in which the desired *E*-isomer predominated ≥20:1 (Scheme 2). Selective acid-catalyzed deprotection of the *tert*-butyl ester (98%) followed by Friedel−Crafts acylation effected by treatment with Ac_2O−NaOAc (reflux, 1 h) provided a mixture of **12**−**15**. Subsequent hydrolysis of the *O*-acetates (K_2CO_3, EtOH) provided **15** (68% overall) and **13**. Notably, the reaction time required for completion of the Friedel−Crafts acylation was significantly reduced with use of the pure *E*-isomer of **11**, and the yield of **15** improved as well. Moreover, this permitted the use of milder Friedel−Crafts reaction conditions (Ac_2O, 1.1 equiv of NaOAc, 70 °C, 10 h) and this modification further improved the ratio of **15**:**13** (8:1). Following this protocol, **15** was isolated

Scheme 3

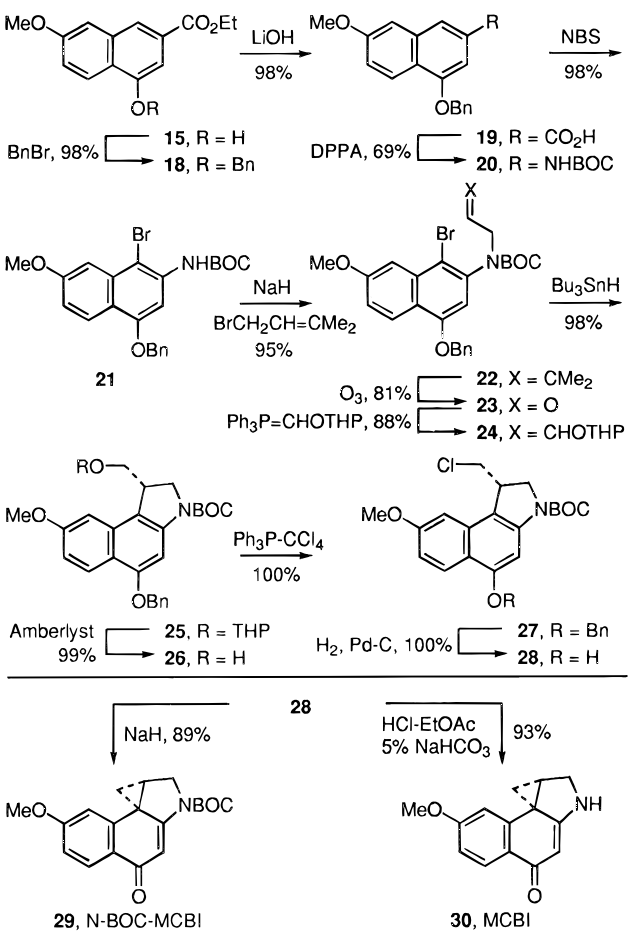

in 76% overall yield from **11**. Similarly, treatment of **11** with TFAA−NaOAc[49] (reflux, 30 h, 57%) provided **15** in slightly lower conversions as a 9:1 mixture of **15**:**13**. Alternative efforts to first convert **11** to the corresponding acid chloride (2 equiv of $(COCl)_2$) followed by Lews acid-catalyzed cyclization ($AlCl_3$, 38%; $FeCl_3$, 46%; $SnCl_4$, 54%) did not improve on these conversions. Not only was the overall conversion of **10** to **15** improved using this modification of the Stobbe condensation but the ability to isolate and characterize pure intermediates in route to **15** permitted an accurate assessment and optimization of each reaction step.

Protection of the phenol **15** as its benzyl ether **18** (98%) followed by hydrolysis of the ethyl ester (98%) and Curtius rearrangement of the resulting carboxylic acid **19** employing the Shioiri−Yamada reagent (DPPA)[53] in *t*-BuOH provided the carbamate **20** directly in excellent conversions (69%, Scheme 3). Low-temperature, acid-catalyzed C4 bromination of **20** (1.2 equiv of NBS, cat. H_2SO_4, THF, −78 °C, 5 h, 98%) cleanly provided **21** whose structure was confirmed with observation of a diagnostic C3-H/OCH_2Ph NOE crosspeak in the 2D $^1H-^1H$ NMR spectrum. Alkylation of the sodium salt of **21** (1.3 equiv of NaH, DMF, 25 °C, 30 min) with 1-bromo-3-methyl-2-butene (3 equiv, DMF, 25 °C, 8 h, 95%) followed by a carefully monitored, low-temperature ozonolysis of **22** and subsequent reductive workup (Me_2S) of the crude ozonide provided **23** (81%). In the optimization of the ozonolysis reaction, the use of more extended reaction

(46) Horning, E. C.; Walker, G. N. *J. Am. Chem. Soc.* **1952**, *74*, 5147.
(47) Edwards, J. D., Jr.; Cashaw, J. L. *J. Am. Chem. Soc.* **1957**, *79*, 2283.
(48) Daub, G. H.; Johnson, W. S. *J. Am. Chem. Soc.* **1950**, *72*, 501.
(49) Bonnett-Delpon, D.; Cambillau, C.; Charpentier-Morize, M.; Jacquot, R.; Mesureur, D.; Ourevitch, M. *J. Org. Chem.* **1988**, *53*, 754.
(50) Guy, A.; Guette, J.-P. *Synthesis* **1980**, 222.
(51) Eaton, P. E; Carlson, G. R.; Lee, J. T. *J. Org. Chem.* **1973**, *38*, 4071.
(52) Owten, W. M.; Gallagher, P. T.; Juan-Montesinos, A. *Synth. Commun.* **1993**, *23*, 2119. Gallagher, P. T.; Hicks, T. A.; Lightfoot, A. P.; Owten, W. M. *Tetrahedron Lett.* **1994**, *35*, 289. Hughes, A. B.; Sargent, M. V. *J. Chem. Soc., Perkin Trans. 1* **1989**, 449. Comber, M. F.; Sargent, M. V. *J. Chem. Soc., Perkin Trans. 1* **1991**, 2783.

(53) Shioiri, T.; Ninomiya, K.; Yamada, S. *J. Am. Chem. Soc.* **1972**, *94*, 6203. Ninomiya, K.; Shioiri, T.; Yamada, S. *Tetrahedron* **1974**, *30*, 2151.

times without an immediate, low-temperature quench of excess O_3 was found to lead to the rapid generation of a further oxidation product. Consequently, adherence to the reaction conditions and particularly the reaction time detailed were critical to the success of the conversion of **22** to **23**. Wittig introduction of the vinyl ether **24** proved most effective with low-temperature generation of $Ph_3P{=}CHOTHP$[54] in THF followed by reaction with **23** in THF−HMPA[55] over a sustained reaction period and provided a mixture of *E*:*Z* olefin isomers in excellent yield (88%). Treatment of **24** with Bu_3SnH (2 equiv, C_6H_6, cat. AIBN, 80 °C, 2 h, 95−98%) provided **25**, the product of 5-*exo-trig* aryl radical−alkene cyclization, in superb yield. Subsequent THP deprotection[56] of **25** provided the free alcohol **26** (99%) and was accomplished without evidence of *N*-BOC deprotection. Conversion of **26** to the primary chloride **27** (2 equiv of Ph_3P, 6 equiv of CCl_4, CH_2Cl_2, 25 °C, 20 h, 99−100%)[57] followed by transfer hydrogenolysis[58] of the benzyl ether (99−100%) and subsequent spirocyclization effected by treatment of **28** with NaH (3 equiv, THF, 0 °C, 30 min, 89%) provided *N*-BOC-MCBI (**29**). Similarly, acid-catalyzed deprotection of **28** (3 N HCl−EtOAc, 25 °C, 20 min) followed by spirocyclization of the crude indoline hydrochloride salt upon exposure to 5% aqueous $NaHCO_3$−THF (1:1, 25 °C, 1.5 h, 93%) cleanly provided MCBI (**30**).

Subsequent to the completion of this synthesis of **29** and **30**, alternative methods to effect the key 5-*exo-trig* aryl radical−alkene cyclization were investigated.[27] In our initial approach, the cyclization of the enol ether **24** proceeded in excellent conversion in part due to the use of an activated acceptor alkene which accelerates the rate of ring closure and reinforces the inherent preference for 5-*exo-trig* cyclization. In addition, the vinyl ether incorporates into the cyclization substrate the full functionalization required in the desired cyclization product. However, the natural limitation of this approach is the requirement to incorporate the product functionality into the acceptor alkene of the free radical cyclization substrate and this entailed a carefully defined ozonolysis reaction and subsequent Wittig reaction with a functionalized methylenetriphenylphosphorane. A shorter and more efficient preparation of **26** was accomplished on the basis of the successful Tempo trap[27] of an aryl radical−alkene 5-*exo-trig* cyclization of an unactivated alkene that precludes the need for alkene functionalization prior to cyclization. Selective, acid-catalyzed C4 iodination of **20** effected by low-temperature treatment with NIS (1.1 equiv, cat. TsOH, THF−CH_3OH, −78 °C, 3 h, 89%) followed by alkylation of the sodium salt of **31** (1.25 equiv of NaH, DMF, 0 °C, 50 min) with allyl bromide (3 equiv, DMF, 25 °C, 3h, 93%) provided **32** (Scheme 4). Treatment of a mixture of **32** and Tempo (6 equiv) in benzene with Bu_3SnH (5 × 1.0 equiv, 70 °C, 1 h) provided **33** (82%) cleanly. Similarly, treatment of **32** and Tempo (6 equiv) in toluene with $(Me_3Si)_3SiH$ (5 × 1 equiv, 80 °C, 10 h) provided **33** (84%) in a reaction that required slightly longer reaction times for completion. Tempo hydrogen atom abstraction from Bu_3SnH or $(Me_3Si)_3SiH$ (Bu_3SnH > $(Me_3Si)_3SiH$) presumably serves to initiate the reaction cascade of tributyltin radical abstraction of iodide from

Scheme 4

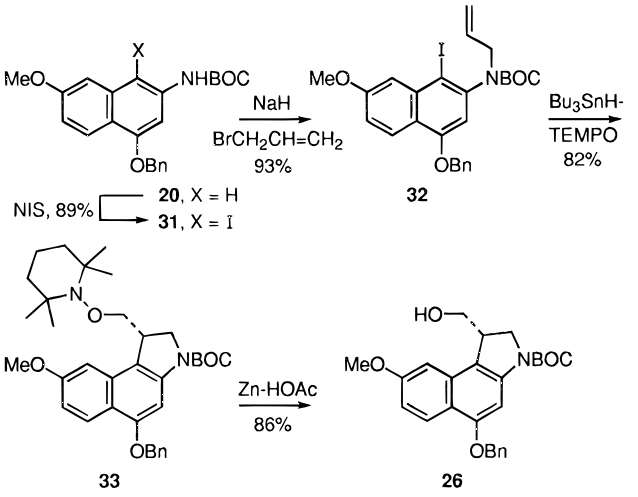

32, 5-*exo-trig* aryl radical−alkene cyclization which proceeds at an exceptionally fast rate[27] and suffers no competitive reduction or intermolecular Tempo trap, and final Tempo trap of the cyclization product primary radical without competitive hydrogen atom abstraction from Bu_3SnH. The competitive reaction of tributyltin radical with Tempo versus **32** presumably accounts for the requirements for excess Bu_3SnH (3−5 equiv) and Tempo (6 equiv). Reductive cleavage of **33** to provide **26** was effected by treatment with Zn (12 equiv, 3:1:1 HOAc−THF−H_2O, 70 °C, 2 h, 86%).

Resolution. The advanced synthetic intermediate **28**, the penultimate intermediate to the MCBI-based analogs, was directly and efficiently resolved on an analytical or semipreparative Daicel Chiralcel OD column ($\alpha = 1.17$).[36] This convenient procedure which avoids diastereomeric derivatization, separation, and dederivatization was found to be best conducted with **28** although **27** ($\alpha = 1.12$) and *N*-BOC-MCBI (**29**, $\alpha = 1.16$) were also capable of direct resolution on a Chiralcel OD column. For our purposes, **28** could be separated on a semipreparative 10 μm, 2 × 25 cm OD HPLC column (2% *i*-PrOH−hexane, 5 mL/min) with a 90−100% recovery of the total sample. Conversion of natural (1*S*)- and *ent*-(1*R*)-**28** to (+)- and *ent*-(−)-*N*-BOC-CBI (**29**) and (+)- and *ent*-(−)-CBI (**30**) followed the experimental procedures detailed in Scheme 3.

The assignment of the absolute configuration was based initially on the relative cytotoxic potencies of natural (+)- and *ent*-(−)-*N*-BOC-MCBI and related analogs, with the former exhibiting more potent activity consistent with observations made with **4**−**9**. This was unambiguously established in a study of the DNA alkylation selectivity of the enantiomers of the advanced analogs **39**−**46**. Consistent with these assignments, the characteristic sign of rotation for the natural and unnatural enantiomers of *N*-BOC-MCBI and MCBI as well as those of the advanced analogs were found to be the same as those observed with **4**−**7** and **9** and their advanced analogs.

MCBI−TMI (40), MCBI−Indole$_2$ (42), MCBI−CDPI$_1$ (44), and MCBI−CDPI$_2$ (46). The MCBI alkylation subunit was incorporated into the CC-1065 and the duocarmycin analogs as detailed in Scheme 5. Acid-catalyzed deprotection of **28** (4 M HCl−EtOAc, 25 °C, 30 min) followed by immediate coupling of the unstable amine hydrochloride salt **34** with 5,6,7-trimethoxyindole-

(54) Schlude, H. *Tetrahedron* **1975**, *31*, 89.
(55) Corey, E. J.; Arai, Y.; Mioskowski, C. *J. Am. Chem. Soc.* **1979**, *101*, 6748.
(56) Bongini, A.; Cardillo, G.; Orena, M.; Sandri, S. *Synthesis* **1979**, 618.
(57) Hooz, J.; Gilani, S. S. H. *Can. J. Chem.* **1968**, *46*, 86.
(58) Beig, T.; Szeja, W. *Synthesis* **1985**, 76.

Scheme 5

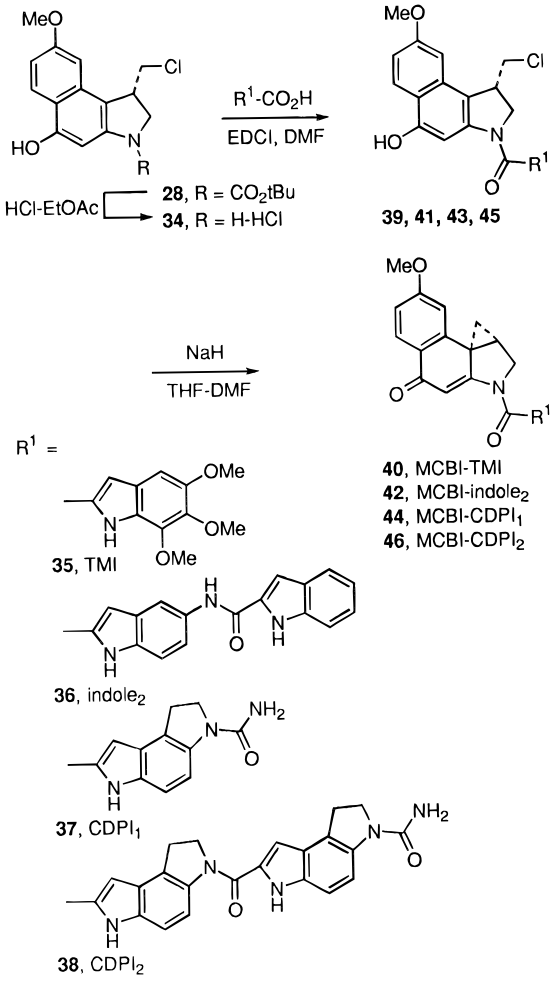

2-carboxylic acid (**35**,[5] 3 equiv of EDCI, DMF, 25 °C, 10 h, 85%), **36**[40] (3 equiv of EDCI, DMF, 25 °C, 10 h, 78%), $CDPI_1$[59] (**37**, 3 equiv of EDCI, DMF, 25 °C, 12 h, 71%), and $CDPI_2$[59] (**38**, 3 equiv of EDCI, DMF, 25 °C, 6 h, 68%) deliberately conducted in the absence of added base which promotes competitive closure of **34** to **30** provided the immediate precursors **39**, **41**, **43**, and **45**, respectively. Notably, the ease of the couplings of **34** with the carboxylic acids **35**−**38** diminished as their solubility decreased (**35**, **36** > **37** > **38**) which necessarily slows the rate of reaction. Subsequent treatment of the coupled agents with NaH (3.0 equiv, THF−DMF 3:1, 0 °C, 30 min) provided MCBI−TMI (**40**, 90%), MCBI−$indole_2$ (**42**, 86%), MCBI−$CDPI_1$ (**44**, 90%), and MCBI−$CDPI_2$ (**46**, 94%), respectively, in excellent conversions. Optimal conversions were observed when the workup of the spirocyclization reaction was conducted with an aqueous phosphate buffer (0.2 M, pH 7) at low temperature (0 °C). Under these conditions the adventitious hydrolysis to MCBI (**30**) was minimized.

Chemical Solvolysis: Reactivity. Two fundamental characteristics of the alkylation subunits have proven important in the studies of **4**−**9** to date. The first is the stereoelectronically-controlled acid-catalyzed ring opening of the activated cyclopropane which dictates preferential addition of a nucleophile to the least-substituted cyclopropane carbon. The second is the relative rate of acid-catalyzed solvolysis which has been found to accurately reflect the functional reactivity of the agents and to follow a fundamental, direct relationship between solvolysis stability and in vitro cytotoxic potency.[21,25,35]

Table 1

agent	k (s^{-1}, pH 3)[a]	$t_{1/2}$ (h, pH 3)[a]	IC_{50} (μM, L1210)	UV, λ_{max} nm (ϵ)	IR (C=O, cm^{-1})
5	1.08×10^{-6}	177	0.006	339 (18000)[b] 301 (14000) 255 (10000)	1719, 1610[c]
4	1.45×10^{-6}	133[g]	0.08	300 (19000)[d] 264 (5700)	1718, 1628 1602[e]
29	1.75×10^{-6}	110[h]	0.09	301 (25000)[d] 270 (20000) 312 (18000)[b] 275 (16000)	1724, 1622 1599[e]
6	5.26×10^{-6}	37	0.3	344 (12000)[b] 278 (17000)	1725, 1570[f]
7	1.75×10^{-5}	11	1	nd	nd
8	9.07×10^{-5}	2.1	2	314 (19000)[b] 260 (9000) 218 (17000)	1705, 1639 1604[c]
9	1.98×10^{-2}	0.01	18	294 (14000)[d] 258 (21000)	1705, 1617[c]

[a] pH = 3: 50% CH_3OH−buffer, buffer is 4:1:20 (v:v:v) 0.1 M citric acid, 0.2 M Na_2HPO_4, and H_2O, respectively. [b] CH_3OH. [c] KBr. [d] THF. [e] Film. [f] Nujol. [g] At pH 2, $k = 1.53 \times 10^{-5}$ s^{-1}, $t_{1/2}$ = 12.5 h. [h] At pH 2, $k = 1.62 \times 10^{-5}$ s^{-1}, $t_{1/2}$ = 11.5 h. [i] nd = not determined.

Provided the C7 substitution of the CBI nucleus would not perturb the stereoelectronic effects on the acid-catalyzed ring opening, this subtle structural change of introducing a C7 methoxy substituent was anticipated to increase the solvolytic reactivity of the agents through electronic activation of C4 carbonyl protonation required of solvolysis. Moreover, it was anticipated that solvolysis would still occur with exclusive cleavage of the C8b−C9 bond with addition of a nucleophile to the least-substituted C9 cyclopropane carbon rather than by cleavage of the C8b−C9a bond with ring expansion and addition of a nucleophile to C9a. Notably, the latter cleavage would place the developing positive charge on a preferred secondary versus primary center, and with preceding agents this preference was overridden by the inherent stereoelectronic control.

Consistent with expectations, *N*-BOC-MCBI (**29**, $t_{1/2}$ = 110 h, $k = 1.75 \times 10^{-6}$ s^{-1}) proved to be more reactive toward chemical solvolysis at pH 3 than *N*-BOC-CBI (**4**, $t_{1/2}$ = 133 h), but the difference was much less pronounced than most might anticipate and **29** was still substantially more stable than *N*-BOC-CPI (**6**, $t_{1/2}$ = 36.7 h), Table 1. Thus, *N*-BOC-MCBI exhibits a half-life only 0.8 times that of the parent agent *N*-BOC-CBI (**4**) at pH 3. Similarly, the solvolysis rate constants were also measured at pH 2 where the reaction was faster and more accurately monitored. At pH 2, the difference was even smaller with *N*-BOC-MCBI (**29**, $t_{1/2}$ = 11.8 h, $k = 1.62 \times 10^{-5}$ s^{-1}) exhibiting a slightly faster solvolysis rate (1.06×) than *N*-BOC-CBI (**4**, $t_{1/2}$ = 12.5 h, $k = 1.53 \times 10^{-5}$ s^{-1}). At pH 7 (1:1 H_2O−CH_3OH) where **4**−**7** show no evidence of solvolysis when monitored for 1−2 weeks, *N*-BOC-MCBI (**29**) similarly did not show evidence of solvolysis. The solvolysis was followed spectrophotometrically by UV with the disappearance of the long-wavelength absorption band of the MCBI chromophore (324 nm) and with the appearance of a short-wavelength absorption band (266 nm) attributable to seco-*N*-BOC-MCBI. Like CPI and CBI, MCBI (**30**, $t_{1/2}$ = 334 h, $k = 5.76 \times 10^{-7}$ s^{-1}) proved substantially more stable to solvolysis than *N*-BOC-MCBI (**29**) and this is presumably the result of preferential N^3-protonation versus *O*-pro-

(59) Boger, D. L.; Coleman, R. S.; Invergo, B. J. *J. Org. Chem.* **1987**, *52*, 1521. Boger, D. L.; Coleman, R. S. *J. Org. Chem.* **1984**, *49*, 2240.

tonation that is required for solvolysis catalysis. Nearly identical to the trends exhibited by **4**−**9**, MCBI (**30**, $t_{1/2}$ = 334 h, $k = 5.76 \times 10^{-7}$ s^{-1}) proved to be only slightly more reactive than CBI ($t_{1/2}$ = 930 h, $k = 2.07 \times 10^{-7}$ s^{-1})[25] and 6−7× more reactive than DSA ($t_{1/2}$ = 2150 h, $k = 8.9 \times 10^{-8}$ s^{-1})[16] but less reactive than CPI.

Thus, the rate of acid-catalyzed solvolysis of *N*-BOC-MCBI (**29**) was predictably faster than that of *N*-BOC-CBI (**4**) due to the electronic activation by the C7 methoxy substituent, but the magnitude of this effect is remarkably small (1.2−1.06×) and revealing. Using the σ_p value of −0.28 for the methoxy substituent,[60] this provides a remarkably small ρ value of −0.30 for the acid-catalyzed solvolysis reaction. Although many mechanistic interpretations of ρ are acknowledged, the most general states that it is a measure of the charge seen by the substituent in the reaction[61] but encompasses other factors including the electron demand,[62] the charge delocalization,[63] the transition state position,[64] and transmission of substituent effects for the reaction under study.[65] Since these factors are not independent, it is not often possible to distinguish the effects. However, an unusually small negative ρ value of −0.3 may be taken to indicate little differential positive charge buildup at the reaction center and suggests a strict S_N2 mechanism for ring opening. Qualitatively, this is easily appreciated by recognizing that the strong electron-donating C7 methoxy substituent of **29** has only a very small 1.2−1.06-fold effect on the rate of acid-catalyzed solvolysis. Like analogous studies of the acid-catalyzed hydrolysis of $XC_6H_4CO_2R$, this clearly indicates that C4 carbonyl protonation is not the rate-determining step of solvolysis but rather nucleophilic addition to the activated cyclopropane (eq 1). No doubt this contributes to the DNA alkylation selectivity of this class of agents and suggests that the positioning of an accessible nucleophile (adenine N3) and not C4 carbonyl protonation or Lewis acid complexation is the rate-determining step controlling the sequence selectivity of DNA alkylation.

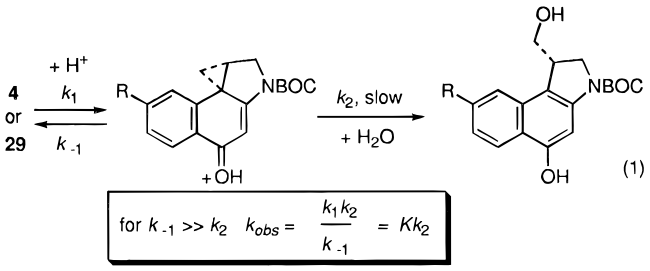

Chemical Solvolysis: Regioselectivity. Treatment of *N*-BOC-MCBI (**29**) with 0.1 equiv of CF_3SO_3H in CH_3OH (0 °C, 3 h) resulted in the clean solvolysis to provide a single product, **47** (95%), eq 2. No *N*-BOC deprotection or olefin was observed, and the methanolysis proceeded without alteration of the stereoelectronically-controlled regioselectivity. Clean cleavage of the C8b−C9 bond with addition of CH_3OH to the least-substituted C9 cyclopropane carbon to provide **47** was observed, and no cleavage of the C8b−C9a bond with ring expansion and addition of CH_3OH to C9a to provide **48** was detected (>20:1). This is in sharp contrast to solvolysis studies of the more reactive alkylation subunits of CC-1065,[66] duocarmycin A,[7] and CBQ[21] where significant amounts of the abnormal ring expansion solvolysis products have been detected, but is consistent with our prior studies of *N*-BOC-CBI (**4**) where no (>20:1) ring expansion solvolysis product was detected.[25] To date the abnormal ring expansion solvolysis products have only been detected with the chemically more reactive agents, *i.e.*, **6**−**8**, and are only especially prevalent in the CBQ system where the stereoelectronic alignment of both cyclopropane bonds are equivalent.[21] Importantly, this stereoelectronically-controlled acid-catalyzed nucleophilic addition to the CBI-based agents including the MCBI-based agents which proceeds with >20:1 regioselectivity provides an additional advantage of the agents over the CPI-based analogs of CC-1065 which have been found to exhibit a more modest 4:1 selectivity.[66]

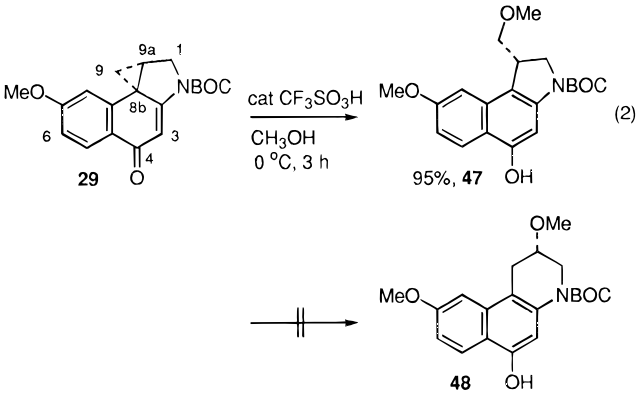

X-ray Structure of MCBI: Structure versus Regioselectivity and Reactivity. The X-ray structure of **30** was determined with cubes grown from 90% EtOAc−CH_3OH and provided the opportunity for comparison directly with the X-ray structure of CBI[25] and related agents (Figure 1). Like CBI, the activated cyclopropane of MCBI was found to be partially, but not fully, conjugated with the cyclohexadienone π-system. The bent orbital of the cyclopropane bond extending to the least-substituted carbon is nearly perpendicular to the plane of the cyclohexadienone and consequently overlaps nicely with the developing π-system of the alkylation product phenol. In contrast, the cyclopropane bond extending to the tertiary carbon and its orbital are nearly orthogonal to the π-system. Thus, opening of the cyclopropane occurs under stereoelectronic control with addition of a nucleophile to the least-substituted carbon, and this stereoelectronic control overrides the intrinsic electronic preference for ring expansion ring opening. Moreover, this is nearly idealized with the CBI and MCBI nucleus and is less effectively accomplished with other subunits examined by X-ray to date including CPI[2] and CBQ.[21]

The cyclopropane ring opening takes place with cleavage of the weakest (longest) bond with nucleophilic attack at the least-substituted carbon. The alternative addition to the more substituted carbon also suffers destabilizing torsional strain encountered by the incoming nucleophile

(60) March, J. *Advances in Organic Chemistry*, 4th ed.; Wiley: New York, 1992.
(61) Hupe, D. J.; Jencks, W. P. *J. Am. Chem. Soc.* **1977**, *99*, 451.
(62) Tanida, H.; Tsushima, T. *J. Am. Chem. Soc.* **1970**, *92*, 3397. Gassman, P. G.; Fentiman, A. F., Jr. *J. Am. Chem. Soc.* **1970**, *92*, 2549.
(63) Johnson, C. D. *Tetrahedron* **1980**, *36*, 3461. Pross, A. *Adv. Phys. Org. Chem.* **1977**, *14*, 69.
(64) McLennan, D. J. *Tetrahedron* **1978**, *34*, 2331.
(65) Bradamante, S.; Pagani, G. A. *J. Org. Chem.* **1980**, *45*, 105.
(66) Warpehoski, M. A.; Harper, D. E. *J. Am. Chem. Soc.* **1994**, *116*, 7573. Warpehoski, M. A.; Harper, D. E. *J. Am. Chem. Soc.* **1995**, *117*, 2951.

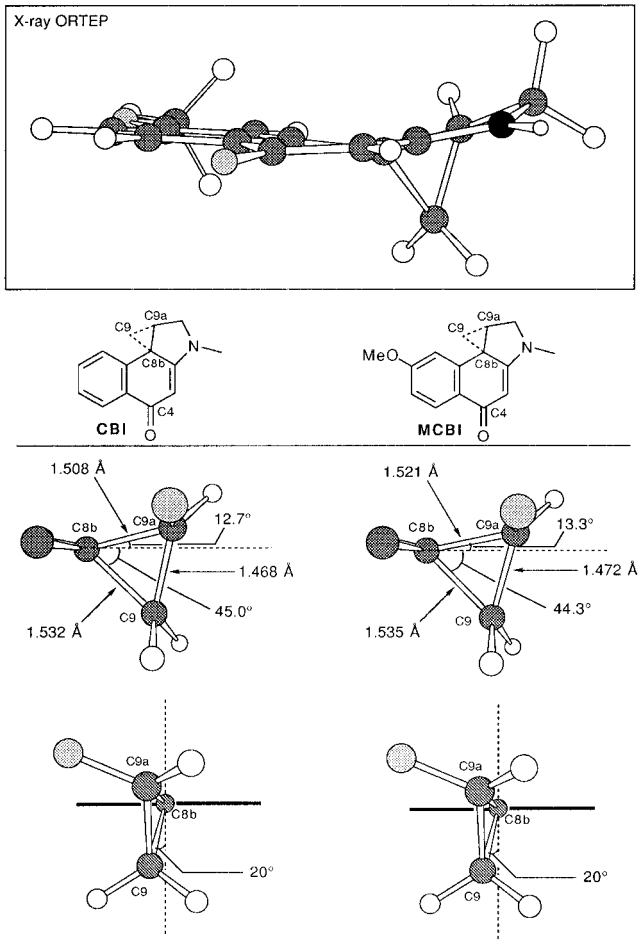

Figure 1. X-ray structure of MCBI and side and rear views of the activated cyclopropane taken from the two X-ray structures highlighting the nonidealized overlap and alignment with the π-system.

which must eclipse a H on the adjacent C1 carbon while attack at the secondary carbon is free of such developing torsional strain. In systems unlike MCBI where there is no stereoelectronic preference for nucleophilic addition, this latter feature has been shown to result in a slight preference for addition to the least-substituted carbon by a mechanism which was unambiguously established to be S_N2.[21]

The constraints of the fused five-membered ring place C9 and C9a at a 20° angle offset from a perfect geometrical alignment and π-overlap with the cyclohexadienone π-system. This nonidealized alignment and conjugation leads to only partial activation of the cyclopropane and productively diminished electrophilic reactivity. Thus, the geometrical constraints of the fused five-membered ring of MCBI and related agents impose stereoelectronic control on nucleophilic cleavage of the cyclopropane, dictating addition to the least-substituted carbon. The nonideal cyclopropane conjugation and alignment with the π-system provide only partial activation and a fine tuned balance between productive electrophilic reactivity and stability.

In Vitro Cytotoxic Activity. A full study of the comparative biological properties of the MCBI-based agents is in progress, and the results of the studies and their correlation with the chemical properties detailed herein will be reported in due course. In preliminary studies, the natural enantiomers of the MCBI-based agents have been found to generally exhibit a cytotoxic potency that is slightly less potent or not distinguishable from that of the corresponding CBI-based agent (Table 2). Although the magnitude of the reactivity differences are small and the variabilities in the cytotoxic assays are large enough to preclude a critical comparison of the CBI and MCBI agents, the qualitative trends are those expected. Importantly and consistent with their relative reactivity, the agents were found to follow the well-established direct relationship between functional stability and cytotoxic potency within the full set of agents and the larger reactivity range that have been examined to date (Figure 2). Analogous to prior observations, the corresponding seco precursors **28**, **39**, **41**, **43**, and **45** exhibited cytotoxic activity indistinguishable from the cyclopropane-containing agents.[67]

Table 2. In Vitro Cytotoxic Activity

agent		IC_{50} (L1210)	agent	IC_{50} (L1210)
	Natural Enantiomers			
29	(+)-*N*-BOC-MCBI	90 nM	(+)-*N*-BOC-CBI	80 nM
40	(+)-MCBI−TMI	8 pM	(+)-CBI−TMI	30 pM
42	(+)-MCBI−indole$_2$	10 pM	(+)-CBI−indole$_2$	10 pM
44	(+)-MCBI−CDPI$_1$	6 pM	(+)-CBI−CDPI$_1$	5 pM
46	(+)-MCBI−CDPI$_2$	6 pM	(+)-CBI−CDPI$_2$	5 pM
	Unnatural Enantiomers			
29	(−)-*N*-BOC-MCBI	200 nM	(−)-*N*-BOC-CBI	900 nm
40	(−)-MCBI−TMI	400 pM	(−)-CBI−TMI	2000 pM
42	(−)-MCBI−indole$_2$	30 pM	(−)-CBI−indole$_2$	4000 pM
44	(−)-MCBI−CDPI$_2$	10 pM	(−)-CBI−CDPI$_1$	380 pM
46	(−)-MCBI−CDPI$_2$	10 pM	(−)-CBI−CDPI$_2$	40 pM

DNA Alkylation Selectivity, Efficiency, and Relative Rates. The DNA alkylation properties of the agents were examined within four 150 base-pair segments of duplex DNA for which comparative results are available for related agents. Four clones of phage M13mp10 were selected for study and contain the SV40 nucleosomal DNA inserts w794 (nucleotide no. 5238-138) and its complement w836 (nucleotide no. 5189-91) and c988 (nucleotide no. 4359-4210) and its complement c820 (nucleotide no. 4201-4356).[10] The alkylation site identification and the assessment of the relative selectivity among the available sites were obtained by thermally-induced strand cleavage of the singly 5′ end-labeled duplex DNA after exposure to the agents. Following treatment of the end-labeled duplex DNA with a range of agent concentrations, the unbound agent was removed by EtOH precipitation of the DNA. Redissolution of the DNA in aqueous buffer, thermolysis (100 °C, 30 min) to induce strand cleavage at the sites of DNA alkylation, denaturing high-resolution polyacrylamide gel electrophoresis (PAGE) adjacent to Sanger dideoxynucleotide sequencing standards, and autoradiography led to identification of the DNA cleavage and alkylation sites. The full details of this procedure have been disclosed and discussed elsewhere.[10] The DNA alkylation reaction selectivities observed under the incubation conditions of 25 °C (24 h) for the agents detailed herein have proven identical to the alkylation selectivities observed with shorter or extended reaction periods or when the reactions were conducted at different temperatures (37 or 4 °C, 0.5−7 d). As discussed below, the rates and efficiencies but not final relative efficiencies of DNA alkylation were altered by changing the reaction temperatures.

DNA Alkylation Properties of the Natural Enantiomers of MCBI−TMI (40), MCBI−Indole$_2$ (42),

(67) (+)- and *ent*-(−)-MCBI (**30**) exhibit IC_{50} (L1210) values of 5 and 30 μM, respectively.

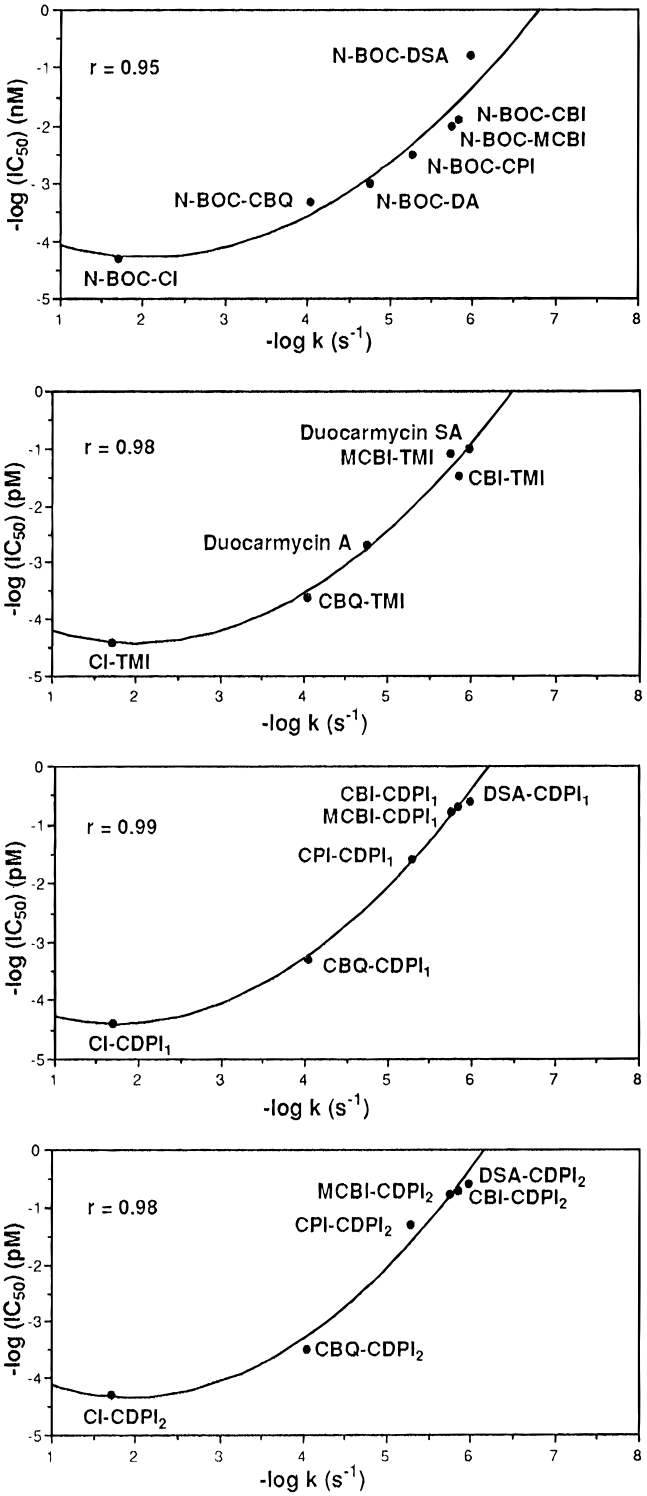

Figure 2.

MCBI−CDPI$_1$ (44), and MCBI−CDPI$_2$ (46). A comparison of the DNA alkylation by the natural enantiomers of **40**, **42**, **44**, and **46** alongside the natural products (+)-duocarmycin SA (**2**) and (+)-CC-1065 (**1**) within w794 DNA is illustrated in Figure 3 and is representative of the full set of comparisons that have been made with the agents. In the comparisons, (+)-duocarmycin SA (**2**) and (+)-MCBI−TMI (**40**) were indistinguishable and the two agents exhibited the same selectivity and efficiency of DNA alkylation. This is illustrated nicely within w794 DNA in Figure 3 where the two agents detectably alkylate the same high-affinity site of 5′-AATTA at 10^{-6} to 10^{-7} M, both alkylate the three additional minor sites to comparable extent only at higher concentrations, and both exhibit the same extent of alkylation throughout the concentration range examined. This is exactly analogous to the observations made in our prior comparisons of duocarmycin SA (**2**) and CBI-TMI.[36]

Similarly, (+)-MCBI−CDPI$_2$ (**46**) and (+)-CC-1065 (**1**) proved essentially indistinguishable in our comparisons. This is illustrated nicely in Figure 3 with w794 DNA where the two agents detectably alkylate the high-affinity site of 5′-AATTA at 10^{-7} M, both alkylate the additional minor sites to comparable extents at higher agent concentrations, and both exhibit the same extent of alkylation throughout the concentration range examined. This is most apparent in the comparison of the amount of unreacted DNA present at each of the reaction concentrations. Similarly, (+)-MCBI−indole$_2$ (**42**) alkylates DNA detectably at 10^{-7} M.

Although this is not as pronounced within w794 where only subtle distinctions in the alkylation selectivity are observed with the relative efficiencies of alkylation of minor sites, the distinctions between duocarmycin SA/MCBI−TMI versus CC-1065/MCBI−CDPI$_2$ are more evident in the additional segments of DNA examined. In these comparisons and like preceding studies that have been described in detail,[6,9,34] the smaller agents including duocarmycin SA, MCBI−TMI, and MCBI−CDPI$_1$ exhibit a clear 3.5 base-pair AT-rich alkylation selectivity while the longer agents including CC-1065 and MCBI−CDPI$_2$ more strongly prefer the larger 5 base-pair AT-rich alkylation sites. These observations are analogous to those made in the direct comparisons of the CBI-based agents with CC-1065[34] or the duocarmycins,[36] and no features which distinguish the behavior of the natural enantiomers of the MCBI- and CBI-based agents were detected. These alkylation selectivities have been documented and described in detail elsewhere[5,6,9,34,36] and summarized in reviews,[11] and each alkylation site detected was adenine followed by two 5′ A or T bases in a three base-pair site that follows the following preference: 5′-AAA > 5′-TTA > 5′-TAA > 5′-ATA. For the shorter agents MCBI−TMI and MCBI−CDPI$_1$, there was also a strong preference but not absolute requirement for the fourth 5′ base to be A or T versus G or C, and this preference distinguished many of the high versus low affinity sites (*e.g.*, 5′-AAAA). For the longer agent MCBI−CDPI$_2$, not only was there a stronger preference for the fourth base to be A or T but that preference extended to include a fifth 5′ A or T base (*e.g.*, 5′-AAAAA). Thus, like the preceding agents, the MCBI-based agents exhibited AT-rich adenine N3 alkylation selectivities that start at the 3′ adenine N3 alkylation site with agent binding in the minor groove in the 3′→5′ direction covering 3.5 or 5 base pairs.

Analogous to the relative rates of DNA alkylation established for (+)-duocarmycin SA (**1**) and (+)-CBI−TMI at the w794 high-affinity site, 5′-AATTA,[36] the relative rates of DNA alkylation for (+)-duocarmycin SA (**1**), (+)-CBI−TMI, and (+)-MCBI−TMI (**40**) were measured (4 °C, 0−48 h, 10^{-6} M agent concentration) and the three agents proved nearly indistinguishable. (+)-MCBI−TMI was found to alkylate the 5′-AATTA high-affinity site kinetically faster at 4 °C than duocarmycin SA or CBI−TMI although the distinctions are quite small: k(**40**):k(CBI−TMI):k(**2**) = 1.8:1.0:0.9 (Figure 4). Similar relative rates were observed in the prior comparisons of

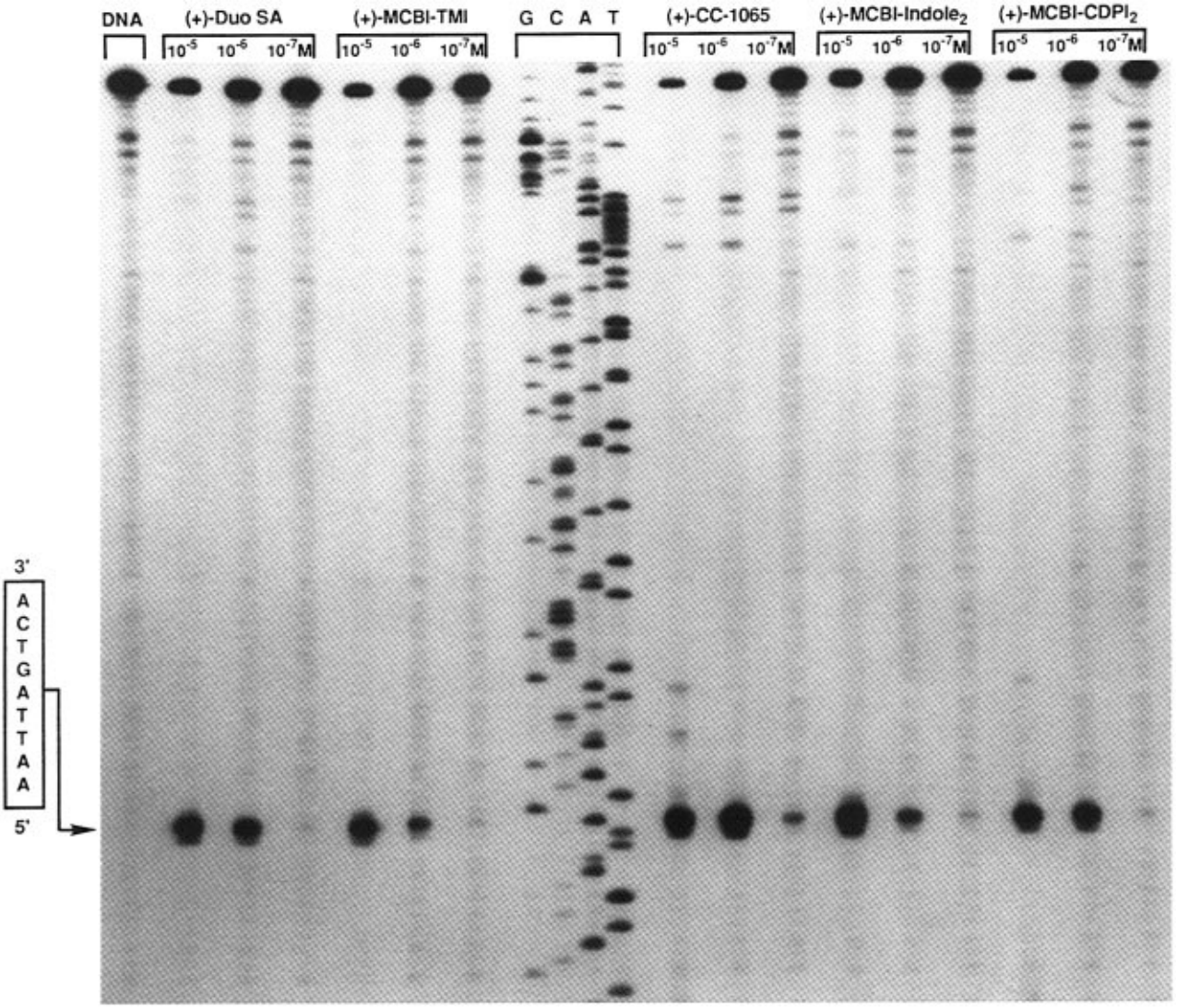

Figure 3. Thermally-induced strand cleavage of double-stranded DNA (SV40 DNA fragment, 144 bp, nucleotide no. 5238-138, clone w794) after 24 h incubation of agent−DNA at 25 °C followed by removal of unbound agent and 30 min incubation at 100 °C; 8% denaturing PAGE and autoradiography. Lane 1, control DNA; lanes 2−4, (+)-duocarmycin SA (**2**, 1×10^{-5} to 1×10^{-7} M); lanes 5−7, (+)-MCBI−TMI (**40**, 1×10^{-5} to 1×10^{-7} M); lanes 8−11, Sanger G, C, A, and T reactions; lanes 12−14, (+)-CC-1065 (**1**, 1×10^{-5} to 1×10^{-7} M); lanes 15−17, (+)-MCBI−indole$_2$ (**42**, 1×10^{-5} to 1×10^{-7} M); lanes 18−20, (+)-MCBI−CDPI$_2$ (**46**, 1×10^{-5} to 1×10^{-7} M).

duocarmycin SA and CBI−TMI, and the three agents are so close that accurate distinctions between CBI−TMI and MCBI−TMI are not readily achievable. At 25 °C, the distinctions are even more difficult to observe and the three agents are essentially indistinguishable, consistent with the relative reactivities of the agents established in the chemical solvolysis studies.

Representative of this difficulty in detecting distinguishing relative rates for the three classes of agents, a similar rate comparison of (+)-DSA−indole$_2$ and (+)-MCBI−indole$_2$ (**42**) conducted at 25 °C (0−24 h) and at 10^{-6} M agent concentration revealed an essentially indistinguishable rate: k(DSA−indole$_2$)/k(MCBI−indole)$_2$ = 1.05 (Figure 4). Importantly, these two comparisons suggest that little if any experimentally distinguishable differences in the relative rates of DNA alkylation are observed with the natural enantiomers of the DSA-, CBI-, or MCBI-based agents. In sharp contrast, all three kinetically alkylate DNA much faster than the corresponding CPI-based agent (10−50×),[30,32,34] where the distinctions are much more pronounced and easily experimentally distinguished.

DNA Alkylation Properties of the Unnatural Enantiomers of MCBI−TMI (40), MCBI−Indole$_2$ (42), MCBI−CDPI$_1$ (44), and MCBI−CDPI$_2$ (46). A representative comparison of the DNA alkylation by the unnatural enantiomers of the MCBI-based agents alongside the unnatural enantiomers of duocarmycin SA (**2**) and CC-1065 (**1**) with the same w794 segment of DNA is illustrated in Figure 5. Several important observations analogous to those made in our prior studies with the CBI-based agents are also observed with the MCBI-based agents. First, the unnatural enantiomer DNA alkylation is considerably slower and the results shown in Figure 5 for the unnatural enantiomers were obtained with incubation at 37 °C (72 h) versus incubation at 25 °C (24 h, Figure 3) for the natural enantiomers. Even with the more vigorous reaction conditions, the extent of alkylation by the unnatural enantiomers is lower, requiring higher agent concentrations for detection. Even longer reaction times at 37 °C were required to achieve the same efficiency of alkylation that was observed with the natural enantiomers at 25 °C (24 h). This distinguishing difference in the rate of DNA alkylation was most

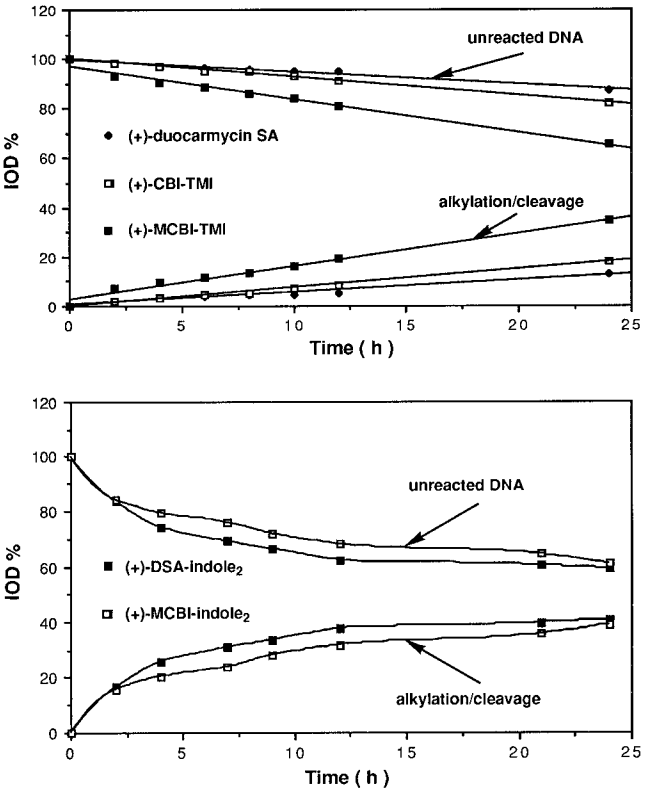

Figure 4. Plot of percent integrated optical density (%IOD) versus time established through autoradiography of 5′-^{32}P end-labeled DNA and used to monitor the relative rate of w794 alkylation of the 5′-AATTA high-affinity site for **2**, **40**, **42**, (+)-CBI−TMI and (+)-DSA−indole$_2$.

prominent with the smaller agents MCBI−TMI (**40**) and duocarmycin SA (**2**), readily perceptible but less prominent with the intermediate-sized agents MCBI−CDPI$_1$ (**44**) and MCBI−indole$_2$ (**42**), and perceptible but even less prominent with the largest agents MCBI−CDPI$_2$ (**46**) and CC-1065 (**1**). This trend is similar to that observed in the relative cytotoxic potency of pairs of enantiomers. (+)-MCBI−TMI is 50× more potent than the corresponding unnatural enantiomer while the natural enantiomers of the larger agents (**42**, **44**, **46**) are only 1−3× more potent, with the enantiomers of **44** and **46** being essentially indistinguishable. This is illustrated nicely in the w794 DNA alkylation in Figure 5 where MCBI−TMI and duocarmycin SA exhibit detectable alkylation at 10^{-5} M, while that of MCBI−CDPI$_1$, MCBI−indole$_2$, and MCBI−CDPI$_2$ are detectable at 10^{-6} to 10^{-7} M. Under the conditions of 25 °C (24 h), the natural enantiomers all alkylate w794 detectably at 10^{-6} to 10^{-7} M (Figure 3).

The DNA alkylation selectivity and efficiency of (−)-MCBI−TMI (**40**) and *ent*-(−)-duocarmycin SA (**2**) were nearly indistinguishable, with the latter agent being slightly more effective. This observation is analogous to that made in our prior comparisons of (−)-CBI−TMI and *ent*-(−)-duocarmycin SA (**2**) except the distinction was larger (10×).[36] Similarly, (−)-MCBI−CDPI$_2$ (**46**) and *ent*-(−)-CC-1065 were nearly indistinguishable as were (−)-MCBI−indole$_2$ and (−)-MCBI−CDPI$_1$. This is perhaps most apparent in comparing the relative extent of labeled DNA consumed at 10^{-5} M in Figure 5. Again, no distinctions in the DNA alkylation selectivity of the unnatural enantiomers of MCBI-based agents and the agents described previously were perceptible. Each of the alkylation sites proved to be adenine which was flanked on both sides nearly always by an A or T base and the preference for this three-base AT-rich site was 5′-AAA > 5′-TAA > 5′-AAT > 5′-TAT. For the shorter agents, there was a strong preference for the second 3′ base to be A or T (*e.g.*, 5′-AAAA) which for the larger agents extended to the third 3′ base as well (*e.g.*, 5′-AAAAA). Thus, each alkylation site for the unnatural enantiomers proved consistent with adenine N3 alkylation with agent binding in the minor groove in the reverse 5′→3′ direction across a 3.5 or 5 base-pair AT-rich site surrounding the alkylation site. This is analogous to the natural enantiomer alkylation selectivity except that it extends in the reverse 5′→3′ direction in the minor groove and, because of the diastereomeric nature of the adducts, is offset by one base-pair relative to the natural enantiomers.

DNA Alkylation Properties of (+)- and *ent*-(−)-*N*-BOC-MCBI. A representative comparison of the DNA alkylation properties of both enantiomers of *N*-BOC-MCBI (**29**) within the same w794 DNA segment is illustrated in Figure 6. No substantial distinctions between *N*-BOC-CBI (**4**) and *N*-BOC-MCBI (**29**) were detected except that the relative efficiency of DNA alkylation by the unnatural enantiomer of **29** was essentially indistinguishable from that of its natural enantiomer under the assay conditions and significantly better than the unnatural enantiomer of *N*-BOC-CBI: (+)-*N*-BOC-CBI/*ent*-(−)-*N*-BOC-CBI (5−10×)[34] versus (+)-*N*-BOC-MCBI/*ent*-(−)-*N*-BOC-MCBI (1−2×). Like the preceding BOC derivatives examined,[5,6,9,10,19,21] the two enantiomers of **29** alkylated DNA much less efficiently than **39**−**46** (10^4×), providing detectable alkylation at 10^{-2} to 10^{-3} M (37 °C, 24−48 h), much less selectively than **39**−**46**, exhibiting a two-base-pair AT-rich alkylation selectivity (5′-AA > 5′-TA), and did so with alkylation of the same sites. This unusual behavior of the two enantiomers alkylating the same sites is analogous to past observations made with **4**−**9**.[11,12] It is a natural consequence of the reversed binding orientations of the two enantiomers and the diastereomeric relationship of the two adducts which result in the two enantiomers covering the exact same binding site surrounding the alkylated adenine. This has been discussed in detail and illustrated elsewhere,[6,9,11,36] and *N*-BOC-MCBI (**29**) conforms nicely to these past observations and models.

Enantiomer Distinctions. Prior studies have suggested an attractive explanation for the confusing behavior of enantiomeric pairs of agents which we have proposed may be attributed to a single structural feature—the degree of steric bulk surrounding the CPI/DSA C7 or CBI/MCBI C8 center in the alkylation subunit for which the unnatural enantiomers are especially sensitive.[6,36] The enantiomer differences have proven distinguishable with simple derivatives of the alkylation subunits themselves (*i.e.*, *N*-BOC-MCBI), are most prominent with the dimer-based agents (*i.e.*, MCBI−TMI), and are less prominent or not readily distinguishable with the larger trimer- or tetramer-based agents (*i.e.*, MCBI−CDPI$_2$). In general, less distinction in the biological potency and relative DNA alkylation efficiency was observed with the CI and duocarmycin SA enantiomeric pairs, both of which lack substituents or steric bulk at this position. Moreover, the distinctions among the enantiomeric CI-based agents which lack the pyrrole ring altogether are small and less pronounced than those observed with the DSA-based agents (DSA > CI). In

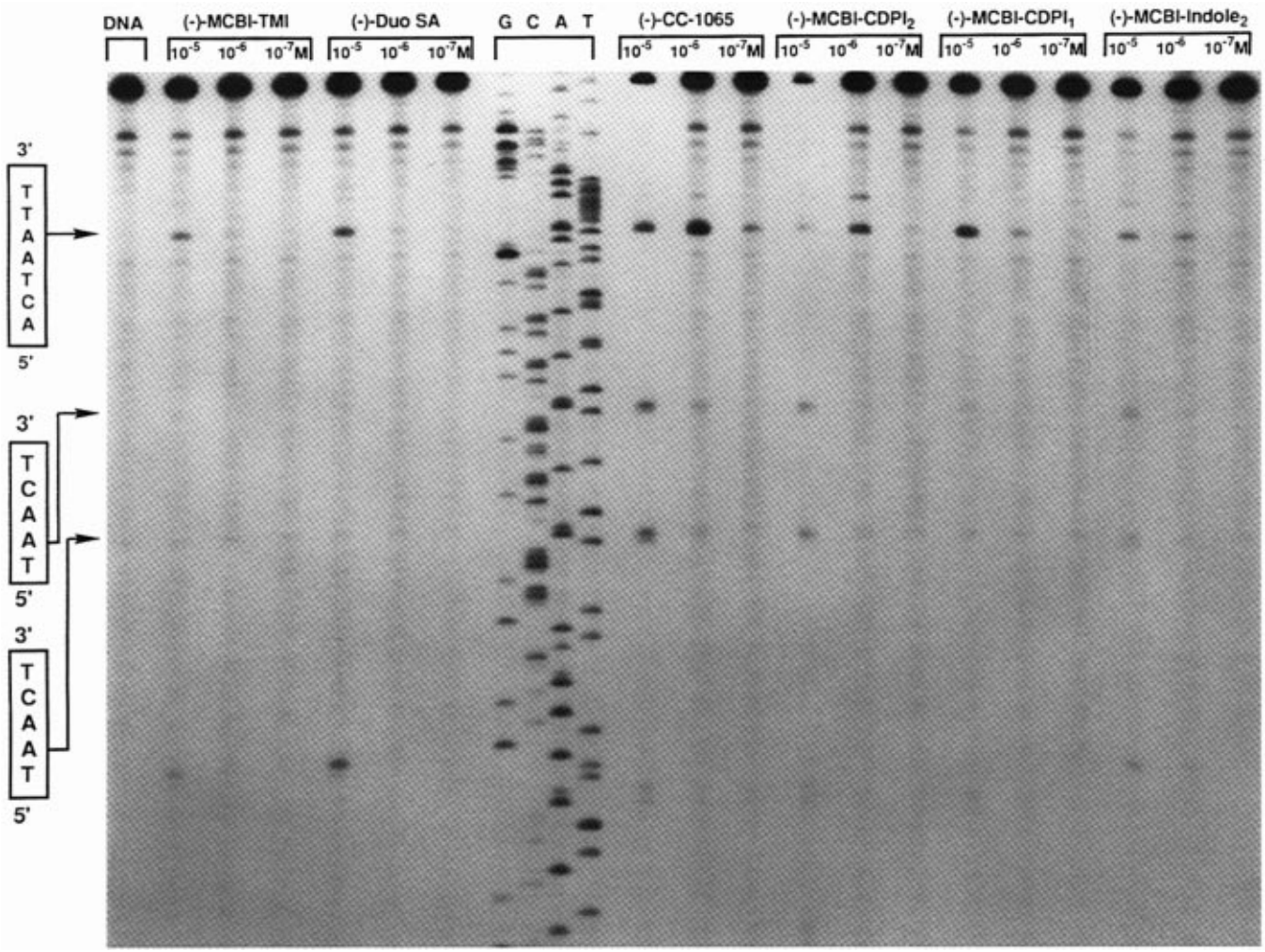

Figure 5. Thermally-induced strand cleavage of double-stranded DNA (SV40 DNA fragment, 144 bp, nucleotide no. 5238-138, clone w794) after 72 h incubation of agent−DNA at 37 °C followed by removal of unbound agent and 30 min incubation at 100 °C; 8% denaturing PAGE and autoradiography. Lane 1, control DNA; lanes 2−4, (−)-MCBI−TMI (**40**, 1×10^{-5} to 1×10^{-7} M); lanes 5−7, (−)-duocarmycin SA (**2**, 1×10^{-5} to 1×10^{-7} M); lanes 8−11, Sanger G, C, A, and T reactions; lanes 12−14, (−)-CC-1065 (**1**, 1×10^{-5} to 1×10^{-7} M); lanes 15−17, (−)-MCBI−$CDPI_2$ (**46**, 1×10^{-5} to 1×10^{-7} M); lanes 18−20, (−)-MCBI−$CDPI_1$ (**44**, 1×10^{-5} to 1×10^{-7} M); lanes 21−23, (−)-MCBI−$indole_2$ (**42**, 1×10^{-5} to 1×10^{-7} M).

contrast, the CPI-, CBI-, and DA-based agents exhibit more pronounced distinctions (CPI > DA > CBI) following an order that reflects the relative steric differences. Consistent with these observations, the MCBI−TMI enantiomers were found to exhibit analogous but smaller distinctions than those observed with CBI−TMI (Table 3). As detailed and illustrated elsewhere,[6,36] this distinguishing behavior of the unnatural enantiomers is derived from a pronounced steric interaction of the CPI/DSA C7 or CBI/MCBI C8 center with the 5′ base adjacent to the adenine N3 alkylation site present in the unnatural enantiomeric 5′→3′ binding model.

Importantly, the only major distinction between the CBI- and MCBI-based agents was observed with the unnatural enantiomers where the MCBI derivatives were found to be 4−40× more potent in cytotoxic assays and more efficient at alkylating DNA than the corresponding CBI derivative. In addition, the unnatural enantiomers of MCBI−$CDPI_1$, MCBI−$indole_2$, and MCBI−$CDPI_2$ were nearly equipotent with the corresponding natural enantiomers in the cytotoxic assays. Although such behavior has been observed with (+)-CC-1065/*ent*-(−)-CC-1065[8,9] and some of the more advanced analogs (*e.g.*, CPI−$CDPI_2$),[9] the unnatural enantiomers of the $indole_2$ and $CDPI_1$ derivatives of various alkylation subunits have been less potent than the natural enantiomers. The comparisons of the cytotoxic properties of the unnatural enantiomers of the CBI derivatives detailed in Table 2 versus those of MCBI−$indole_2$, MCBI−$CDPI_1$, and MCBI−$CDPI_2$ are representative of such past and present observations. In contrast to the CBI-based agents where the unnatural enantiomers were 8−400× less potent than the natural enantiomers with only the two enantiomers of CBI−$CDPI_2$ exhibiting comparable potencies, both enantiomers of MCBI−$indole_2$, MCBI−$CDPI_1$, and MCBI−$CDPI_2$ were comparable in cytotoxic potency (1−3×) and the distinctions essentially absent with the tighter binding $CDPI_1$ and $CDPI_2$ derivatives.

These observations may be important in distinguishing the origin of the biological potencies of this class of reversible DNA alkylating agents. Two proposals have been advanced in which the biological potencies have been suggested to be related to either the rate of DNA alkylation[8,12] or to the thermodynamic stability of the adducts and the resulting relative efficiency of DNA alkylation.[9,11] Clearly not only do the rates of DNA alkylation between the various natural enantiomers of the MCBI derivatives vary widely but the rates of DNA alkylation between the enantiomeric pairs vary to an even larger extent. The near equivalent cytotoxic poten-

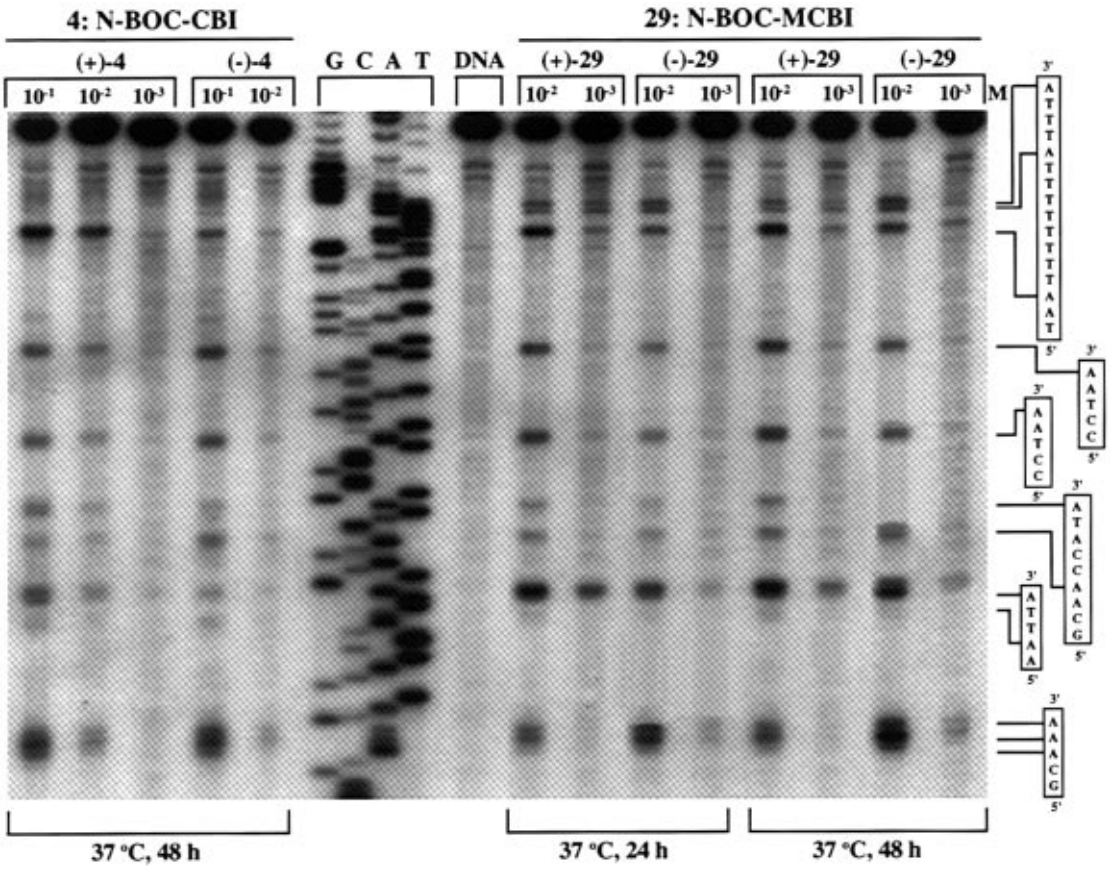

Figure 6. Thermally-induced strand cleavage of 5′ end-labeled DNA (SV40 DNA fragment, 144 bp, nucleotide no. 5238-138, clone w794). As indicated, the DNA−agent incubation was conducted at 37 °C for 24 or 48 h followed by removal of unbound agent and 30 min incubation at 100 °C; 8% denaturing PAGE and autoradiography.

Table 3. Enantiomer Distinctions

agent	rel IC_{50} (L1210)[a]	rel DNA alkylation intensity[b]
CI−TMI	1	0.5−2.0
duocarmycin SA	10	10
MCBI−TMI	50	50
CBI−TMI	100	100
duocarmycin A	>100	>100

[a] IC_{50} (unnatural)/(natural) enantiomer. [b] Concentrations of unnatural/natural enantiomer required to detect DNA alkylation.

cies among the full set of MCBI natural enantiomers and the comparable cytotoxic potency of most of the unnatural MCBI enantiomers is inconsistent with the proposal that the rates of DNA alkylation can be related to cytotoxic potency but is entirely consistent with the proposal that the thermodynamic stability and resulting efficiency of DNA alkylation may be directly related. The unnatural enantiomers form inherently less stable adducts and are more readily reversed than the corresponding natural enantiomers. For the natural enantiomers, a single DNA alkylation subunit is sufficient to provide functionally stable adducts (*i.e.*, TMI, $CDPI_1$) and provides fully potent agents capable of efficient DNA alkylation. For the unnatural enantiomers, the full biological potency and efficient DNA alkylation have generally been achieved only with the agents containing two large DNA binding subunits (*i.e.*, $CDPI_2$). Intermediate potencies are seen with the smaller agents which diminish as their size and noncovalent binding affinity decreases. Representative of such a trend is the behavior of the unnatural enantiomers of the CBI-based agents (Table 2). The unnatural enantiomers of MCBI follow this same trend except that they behave more like the natural enantiomers in that they are more potent and reach a plateau of cytotoxic potency with some of the simpler, single DNA binding subunit derivatives. To us, this has suggested that the C7 methoxy substituent on the alkylation subunit of the MCBI unnatural enantiomers provides sufficient additional noncovalent binding stabilization to enhance the apparent efficiency or stability of the unnatural enantiomer DNA alkylation. Consistent with this proposal, even the *N*-BOC-MCBI and the MCBI−TMI enantiomers were found to exhibit less distinction than those of CBI−TMI. While this impact of a single methoxy group may appear speculative, similar potentiating effects of a single methoxy substituent within the TMI subunit of (+)-duocarmycin SA have been observed.[68] Similarly, the duocarmycin SA C6 methoxycarbonyl group may be contributing to the potentiation of the DSA unnatural enantiomers.[5,6,16]

This interpretation and relationship of the cytotoxic potency with the efficiency of DNA alkylation and stability of the adducts is especially attractive since it is consistent with the direct relationship between cytotoxic potency and functional stability observed with derivatives of **4**−**9**. Consistent with the interpretation that it is not the rate of DNA alkylation and functional reactivity that enhances cytotoxic potency but rather the net efficiency and relative stability of the DNA alkylation process, it is the chemically more stable agents which may most effectively reach their intracellular biological target that

(68) Boger, D. L.; Bollinger, B. Unpublished observations.

exhibit the more potent cytotoxic activity provided they are sufficiently reactive to alkylate DNA with the formation of functionally stable adducts.

Conclusions. A short and efficient 12−13 step (27−30% overall) synthesis of MCBI and its immediate precursors is detailed and constitutes the first substituted CBI derivative disclosed. Its evaluation permitted the first assessment of the electronic effect of substituents on the chemical and functional reactivity of the agents and the impact this may have on their biological properties. A study of the solvolysis reactivity of *N*-BOC-MCBI indicated that the introduction of the strong electron-donating C7 methoxy group accelerates the rate of solvolysis by only 1.2−1.06×. This remarkably small effect indicates that protonation of the C4 carbonyl is not the rate-determining step of solvolysis or acid-catalyzed nucleophilic addition and further supports the proposal that the cyclopropane ring-opening reaction requires the presence and assistance of a nucleophile (S_N2 mechanism). No doubt this contributes to the DNA alkylation selectivity and suggests that the positioning of an accessible nucleophile (adenine N3) and not C4 carbonyl protonation or Lewis acid complexation is the rate-determining step controlling the sequence selectivity of DNA alkylation. This exceptionally small electronic effect on the solvolysis rate had no impact on the solvolysis regioselectivity, and stereoelectronically-controlled nucleophilic addition to the least-substituted carbon of the activated cyclopropane was observed exclusively. For the natural enantiomers, this very small electronic effect on functional reactivity had little or no perceptible effect on their DNA alkylation selectivity, efficiency, and relative rates or on their biological properties when compared to the corresponding CBI-based agent. Perceptible effects of the C7 methoxy group on the unnatural enantiomers were detected, and they proved to be 4−40× more effective than the corresponding CBI-based unnatural enantiomers and comparable in cytotoxic potency with the corresponding MCBI natural enantiomer. This effect on the unnatural enantiomers is most consistently rationalized not by a C7 methoxy substituent effect on functional reactivity but rather through introduction of additional stabilizing noncovalent interactions which increase DNA alkylation efficiency and further stabilize an inherently reversible DNA alkylation reaction.

Experimental Section

Ethyl 1-Hydroxy-6-methoxynaphthalene-3-carboxylate (15). Method A. A solution of *t*-BuOK (21.0 g, 0.19 mol, 2 equiv) in *t*-BuOH (81 mL) was added to a solution of **10** (10.8 mL, 11.8 g, 0.087 mol) and diethyl succinate (40.2 mL, 0.242 mol, 3 equiv), and the mixture was warmed at reflux for 45 min. Additional diethyl succinate (40.2 mL, 0.242 mol, 3 equiv) and *t*-BuOK (21.0 g, 0.19 mol, 2 equiv) in *t*-BuOH (81 mL) were added, and the mixture was warmed at reflux for an additional 45 min. The mixture was cooled, acidified with the addition of 25% aqueous HCl, and extracted with Et_2O (3 × 15 mL). The organic layer was extracted with 5% aqueous Na_2CO_3 (6 × 40 mL). The resulting aqueous phase was acidified with the addition of 25% aqueous HCl and reextracted with Et_2O (3 × 30 mL). The combined organic layer was dried (Na_2SO_4) and concentrated under reduced pressure, providing an oily product that proved to be a 2:1 mixture of the isomeric half-esters **11** (15.0 g, 23.2 g theoretical, 74%).

The mixture of **11** (15.0 g, 64 mmol) was treated with Ac_2O (320 mL) and NaOAc (5.25 g, 64 mmol, 1.0 equiv) and warmed at reflux for 5 h. The solvent was removed under reduced pressure, and the residue was treated with 15% aqueous Na_2CO_3 (100 mL) and extracted with EtOAc (3 × 30 mL). The organic layer was dried (Na_2SO_4) and concentrated in vacuo.

Without further purification, the dark brown oil was dissolved in EtOH (100 mL) and treated with K_2CO_3 (10 g, 72.4 mmol). The mixture was warmed at reflux for 18 h before being cooled, concentrated, diluted with H_2O (40 mL), acidified to pH 6 with the addition of 10% aqueous HCl, and extracted with EtOAc (3 × 20 mL). The organic layer was dried (Na_2SO_4) and concentrated under reduced pressure. Flash chromatography (5 × 20 cm SiO_2, 10−30% EtOAc−hexane gradient elution) afforded **15** (8.90 g, 21.4 g theoretical, 42% for 3 steps) as a white solid: mp 168 °C (hexane, colorless plates); ^{1}H NMR ($CDCl_3$, 400 MHz) δ 8.15 (d, J = 8.8 Hz, 1H, C8-H), 8.10 (s, 1H, C4-H), 7.38 (s, 1H, C2-H), 7.23 (dd, J = 3.2, 8.8 Hz, 1H, C7-H), 7.20 (d, J = 3.2 Hz, 1H, C5-H), 4.40 (q, J = 8.0 Hz, 2H), 3.90 (s, 3H, OCH_3), 1.40 (t, J = 8.0 Hz, 3H); ^{13}C NMR ($CDCl_3$, 100 MHz) δ 166.1, 157.5, 152.9, 134.4, 127.9, 123.3, 121.7, 119.8, 118.6, 106.0, 104.8, 60.0, 54.5, 13.7; IR (KBr) ν_{max} 3385, 1683, 1608, 1397, 1283, 1225, 1028, 878, 833, 768 cm^{-1}; FABHRMS (NBA) m/e 246.0885 (M^+, $C_{14}H_{14}O_4$ requires 246.0892).

Anal. Calcd for $C_{14}H_{14}O_4$: C, 68.28; H, 5.73. Found: C, 68.22; H, 5.77.

Variable amounts of **13** were also isolated. For **13**: mp 88−89 °C; ^{1}H NMR ($CDCl_3$, 400 MHz) δ 9.32 (s, 1H, OH), 8.03 (d, J = 1.5 Hz, 1H, C4-H), 7.50 (d, J = 8.2 Hz, 1H, C5-H), 7.43 (d, J = 1.5 Hz, 1H, C2-H), 7.37 (t, J = 8.2 Hz, 1H, C6-H), 6.86 (d, J = 7.6 Hz, 1H, C7-H), 4.39 (q, J = 7.8 Hz, 2H), 4.09 (s, 3H, OCH_3), 1.39 (t, J = 7.8 Hz, 3H); ^{13}C NMR ($CDCl_3$, 100 MHz) δ 166.5, 155.9, 154.6, 135.8, 129.5, 126.4, 123.1, 121.5, 117.1, 109.6, 106.0, 61.1, 56.2, 14.3; IR (film) ν_{max} 3404, 3056, 2980, 1718, 1711, 1611, 1583, 1468, 1450, 1380, 1290, 1220, 1126, 1087 cm^{-1}; FABHRMS (NBA−NaI) m/e 269.0786 (M^+ + Na, $C_{14}H_{14}O_4$ requires 269.0790).

Anal. Calcd for $C_{14}H_{14}O_4$: C, 68.28; H, 5.73. Found: C, 68.23; H, 5.64.

Method B, from 17. A 9:1 mixture of CF_3CO_2H−H_2O (50 mL) at 0 °C was added to **17** (3.10 g, 9.68 mmol), and the reaction mixture was warmed to 25 °C and stirred for 2 h. The reaction mixture was concentrated in vacuo, and two separate 50 mL volumes of toluene were sequentially added and removed under reduced pressure to provide **11** (2.50 g, 2.56 g theoretical, 98%) as a colorless oil.

A mixture of **11** (2.50 g, 9.46 mmol) and NaOAc (0.750 g, 9.50 mmol) in 50 mL of Ac_2O was warmed at 70 °C for 10 h. The volatiles were removed in vacuo, and a solution of the crude product and K_2CO_3 (1.38 g, 10.0 mmol) in 35 mL of EtOH was warmed at reflux for 4 h. The reaction mixture was cooled to 0 °C, acidified with the addition of 1 M HCl (pH 6), and extracted with Et_2O (4 × 30 mL). The organic layers were combined, washed with saturated aqueous NaCl (1 × 10 mL), dried (Na_2SO_4), and concentrated under reduced pressure. Centrifugal thin-layer chromatography (SiO_2, 4 mm Chromatotron plate, 5−20% EtOAc−hexane gradient elution) provided **15** (1.79 g, 2.33 g theoretical, 76%) and **13** (0.22 g, 9%) as white crystalline solids.

Table 4 summarizes the results of related efforts to convert **11** derived from **17** to **15**.

Table 4

conditions	reaction time (h)	ratio **15**:**13**	% **15** isolated
Ac_2O−NaOAc, 160 °C[a]	1	5:1	61
Ac_2O−NaOAc, 70 °C[a]	10	8:1	76
TFAA−NaOAc, 40 °C[a]	30	9:1	57
$(COCl)_2$; $AlCl_3$, 0 °C	1	11:1	38
$(COCl_2)$; $FeCl_3$, 0 °C	2	10:1	46
$(COCl_2)$; $SnCl_4$, 0 °C	2	11:1	54

[a] Subsequent treatment with K_2CO_3−EtOH.

***tert*-Butyl (*E*)-3-(Ethoxycarbonyl)-4-(3-methoxyphenyl)-3-butenoate (17).** A suspension of NaH (0.64 g, 16 mmol, 60% in oil) in 25 mL of THF was added to a solution of **16**[52] (5.00 g, 14.8 mmol) in 40 mL of THF at 0 °C, and the reaction mixture was warmed to 25 °C and stirred for 10 h. The

solution was cooled to 0 °C, **10** (2.00 g, 14.8 mmol) in 25 mL of THF was added, and the mixture was warmed to 25 °C and stirred for 10 h. A majority of the THF was removed under reduced pressure, and saturated aqueous $NaHCO_3$ (20 mL) was added. The aqueous layer was extracted with EtOAc (4 × 30 mL), and the organic layers were combined, washed with saturated aqueous NaCl, dried (Na_2SO_4), and concentrated in vacuo. Chromatography (SiO_2, 6 × 15 cm, 5−10% EtOAc−hexane gradient elution) provided **17** (3.65 g, 4.74 g theoretical, 77%) as a colorless oil as a single isomer by ^1H NMR (>20:1): ^1H NMR ($CDCl_3$, 400 MHz) δ 7.80 (s, 1H, C2′-H), 7.28 (t, J = 7.8 Hz, 1H, C5′-H), 6.92−6.86 (m, 3H), 4.26 (q, J = 7.1 Hz, 2H), 3.79 (s, 3H, OCH_3), 3.44 (s, 2H, C2-H_2), 1.44 (s, 9H), 1.31 (t, J = 7.1 Hz, 3H); ^{13}C NMR ($CDCl_3$, 100 MHz) δ 170.3, 167.5, 159.6, 141.1, 136.5, 129.5, 127.0, 121.4, 114.7, 114.0, 81.0, 61.0, 55.2, 35.0, 28.0, 14.2; IR (film) 2978, 2933, 1726, 1708, 1578, 1368, 1278, 1194, 1155, 1096 cm^{-1}; FABHRMS (NBA) m/e 321.1716 (M^+ + H, $C_{18}H_{24}O_5$ requires 321.1702).

Anal. Calcd for $C_{18}H_{24}O_5$: C, 67.48; H, 7.55. Found: C, 67.39; H, 7.17.

Ethyl 1-(Benzyloxy)-6-methoxynaphthalene-3-carboxylate (18). A solution of **15** (900 mg, 3.65 mmol) in anhydrous DMF (12.5 mL) under N_2 was treated with anhydrous K_2CO_3 (700 mg, 5.1 mmol, 1.4 equiv), benzyl bromide (0.51 mL, 4.3 mmol, 1.2 equiv), and Bu_4NI (0.7 mg). The mixture was stirred at 25 °C for 5 h before it was concentrated under reduced pressure. Chromatography (SiO_2, 2−5% EtOAc−hexane gradient elution) provided **18** (1.20 g, 1.23 g theoretical, 98%) as a colorless semisolid: ^1H NMR ($CDCl_3$, 400 MHz) δ 8.20 (d, J = 9.6 Hz, 1H, C8-H), 8.10 (s, 1H, C4−H), 7.53 (d, J = 8.0 Hz, 2H), 7.40 (t, J = 8.0 Hz, 1H), 7.37 (d, J = 2.4 Hz, 1H, C5-H), 7.34 (m, 2H), 7.19 (dd, J = 2.4, 9.6 Hz, 1H, C7-H), 7.18 (s, 1H, C2-H), 5.20 (s, 2H, C$H_2C_6H_5$), 4.40 (q, J = 8.0 Hz, 2H), 3.90 (s, 3H, OCH_3), 1.40 (t, J = 8.0 Hz, 3H); ^{13}C NMR ($CDCl_3$, 100 MHz) δ 166.9, 158.6, 154.7, 136.8, 134.9, 128.6, 128.56, 128.3, 128.2, 127.6, 123.9, 122.6, 119.9, 106.9, 102.4, 71.1, 61.1, 55.2, 14.3; IR (film) ν_{max} 2978, 1715, 1603, 1455, 1406, 1366, 1345, 1286, 1237, 1149, 1097, 1029 cm^{-1}; FABHRMS (NBA−CsI) m/e 469.0422 (M^+ + Cs, $C_{21}H_{20}O_4$ requires 469.0416).

Anal. Calcd for $C_{21}H_{20}O_4$: C, 74.98; H, 5.99. Found: C, 75.21; H, 5.91.

1-(Benzyloxy)-6-methoxynaphthalene-3-carboxylic Acid (19). A solution of **18** (2.49 g, 7.40 mmol) in THF−CH_3OH−H_2O (4:1:1, 50 mL) was treated with LiOH−H_2O (930 mg, 22.2 mmol, 3 equiv). The suspension was stirred at 23 °C for 18 h before H_2O (20 mL) was added. The solution was acidified with the addition of 10% aqueous HCl, and the white precipitate was collected. Crystallization from EtOH afforded **19** (2.17 g, 2.28 g theoretical, 95%, typically 95−98%) as white needles: mp 185 °C (EtOH, white needles); ^1H NMR (DMSO-d_6, 400 MHz) δ 8.15 (d, J = 9.6 Hz, 1H, C8-H), 8.10 (s, 1H, C4-H), 7.57 (d, J = 9.6 Hz, 2H), 7.50 (d, J = 2.0 Hz, 1H, C5-H), 7.43 (t, J = 9.6 Hz, 1H), 7.37 (d, J = 9.6 Hz, 2H), 7.34 (s, 1H, C2-H), 7.27 (dd, J = 2.0, 9.6 Hz, 1H, C7-H), 5.30 (s, 2H, C$H_2C_6H_5$), 3.90 (s, 3H, OCH_3); ^{13}C NMR (DMSO-d_6, 100 MHz) δ 167.6, 158.2, 154.1, 136.9, 134.8, 129.0, 128.5, 127.9, 127.5, 123.3, 122.2, 122.1, 120.0, 107.6, 102.6, 69.5, 55.4; IR (KBr) ν_{max} 2932, 2647, 2543, 1685, 1629, 1420, 1296, 1201, 1030, 891, 768, 638 cm^{-1}; FABHRMS (NBA) m/e 308.1040 (M^+, $C_{19}H_{16}O_4$ requires 308.1049).

Anal. Calcd for $C_{19}H_{16}O_4$: C, 74.01; H, 5.23. Found: C, 73.86; H, 5.33.

***N*-(*tert*-Butyloxycarbonyl)-1-(benzyloxy)-6-methoxy-3-naphthylamine (20).** A solution of **19** (1.20 g, 3.91 mmol) in *t*-BuOH (75 mL) was treated sequentially with diphenylphosphoryl azide[53] (DPPA, 1.29 g, 4.69 mmol, 1.2 equiv) and Et_3N (0.67 mL, 4.69 mmol, 1.2 equiv), and the mixture was stirred at reflux for 10 h. The mixture was cooled and concentrated in vacuo. Centrifugal thin-layer chromatography (SiO_2, 4 mm Chromatotron plate, 5−10% EtOAc−hexane gradient elution) afforded **20** (1.01 g, 1.48 g theoretical, 68%, typically 60−69%) as a white solid: mp 138 °C (hexane, white needles); ^1H NMR ($CDCl_3$, 400 MHz) δ 8.10 (d, J = 9.6 Hz, 1H, C8-H), 7.50 (d, J = 8.8 Hz, 2H), 7.40 (m, 2H), 7.35 (m, 2H), 6.98 (d, J = 1.9 Hz, 1H, C4-H), 6.95 (dd, J = 2.5, 9.6 Hz, 1H, C7-H), 6.86 (d, J = 1.9 Hz, 1H, C2-H), 6.65 (s, 1H, NH), 5.20 (s, 2H, C$H_2C_6H_5$), 3.80 (s, 3H, OCH_3), 1.50 (s, 9H); ^{13}C NMR ($CDCl_3$, 100 MHz) δ 158.7, 155.3, 152.7, 136.9, 136.3, 129.8, 128.6, 127.9, 127.4, 123.7, 117.6, 116.0, 106.7, 105.3, 97.2, 80.6, 70.1, 55.2, 28.4; IR (KBr) ν_{max} 3323, 2978, 1698, 1591, 1549, 1422, 1346, 1228, 1148, 1024, 945, 869, 820, 756, 701 cm^{-1}; FABHRMS (NBA−CsI) m/e 512.0846 (M^+ + Cs, $C_{23}H_{25}NO_4$ requires 512.0838).

Anal. Calcd for $C_{23}H_{25}NO_4$: C, 72.80; H, 6.64; N, 3.69. Found: C, 72.42; H, 6.77; N, 3.92.

***N*-(*tert*-Butyloxycarbonyl)-4-(benzyloxy)-1-bromo-7-methoxy-2-naphthylamine (21).** A solution of **20** (620 mg, 1.63 mmol) in THF (35 mL) under N_2 was cooled to −78 °C and treated with a solution of THF (2 mL) containing 10 μL of concentrated H_2SO_4. After 5 min, a solution of NBS (320 mg, 1.80 mmol, 1.1 equiv) in THF (10 mL) was added and the mixture was stirred at −78 °C for 2 h. The mixture was diluted with Et_2O (50 mL), washed with saturated aqueous $NaHCO_3$ (2 × 10 mL) and saturated aqueous NaCl (20 mL), dried (Na_2SO_4), and concentrated in vacuo. Centrifugal thin-layer chromatography (SiO_2, 4 mm Chromatotron plate, 5−10% EtOAc−hexane) afforded **21** (720 mg, 747 mg theoretical, 96%, typically 90−98%) as a white solid: mp: 125−127 °C (hexane, white solid); ^1H NMR ($CDCl_3$, 400 MHz) δ 8.10 (d, J = 9.2 Hz, 1H, C5-H), 7.98 (s, 1H, C3-H), 7.55 (d, J = 7.2 Hz, 2H), 7.40 (m, 5H), 7.02 (dd, J = 2.4, 9.2 Hz, 1H, C6-H), 5.20 (s, 2H, C$H_2C_6H_5$), 3.90 (s, 3H, OCH_3), 1.50 (s, 9H); the 2D ^1H−^1H NOESY NMR ($CDCl_3$, 400 MHz) displayed a diagnostic NOE crosspeak for C3-H/C$H_2C_6H_5$; ^{13}C NMR ($CDCl_3$, 100 MHz) δ 159.8, 154.7, 152.5, 136.6, 135.6, 133.9, 128.6, 128.1, 128.0, 127.8, 124.5, 118.3, 116.3, 105.1, 97.6, 81.2, 70.3, 55.3, 28.6; IR (KBr) ν_{max} 3409, 2977, 1733, 1623, 1506, 1367, 1222, 1153, 1030, 989, 882, 829, 753 cm^{-1}; FABHRMS (NBA) m/e 457.0880 (M^+, $C_{23}H_{24}BrNO_4$ requires 457.0889).

Anal. Calcd for $C_{23}H_{24}BrNO_4$: C, 60.27; H, 5.28; N, 3.06. Found: C, 60.20; H, 5.04; N, 2.99.

2-[*N*-(*tert*-Butyloxycarbonyl)-*N*-(3-methyl-2-buten-1-yl)amino]-4-(benzyloxy)-1-bromo-7-methoxynaphthalene (22). A suspension of NaH (44 mg, 0.92 mmol, 50% in oil, 1.3 equiv) in DMF (4 mL) at 24 °C under Ar was treated with **21** (315 mg, 0.71 mmol), and the reaction mixture was stirred for 30 min. The mixture was cooled to 0 °C, and 4-bromo-2-methyl-2-butene (0.25 mL, 2.1 mmol, 3 equiv) was added slowly. The mixture was allowed to warm to 24 °C and was stirred for 8 h before being poured onto H_2O (15 mL). The mixture was extracted with EtOAc (3 × 10 mL), and the combined organic extracts were washed with H_2O (10 mL) and saturated aqueous NaCl (5 mL), dried (Na_2SO_4), and concentrated in vacuo. Chromatography (SiO_2, 5−7% EtOAc−hexane gradient elution) afforded **22** (357 mg, 374 mg theoretical, 95%) as an off-white solid: mp 108−109 °C (hexane, white solid); ^1H NMR ($CDCl_3$, 400 MHz) mixture of amide rotamers, for the major rotamer δ 8.10 (d, J = 9.2 Hz, 1H, C5-H), 7.56 (d, J = 2.4 Hz, 1H, C8-H), 7.47 (d, J = 7.2 Hz, 2H), 7.38 (m, 3H), 7.13 (dd, J = 2.4, 9.2 Hz, 1H, C6-H), 6.55 (s, 1H, C3-H), 5.30 (t, J = 6.8 Hz, 1H, CH=C), 5.20 (d, J = 11.7 Hz, 1H, CHHC$_6$H$_5$), 5.14 (d, J = 11.7 Hz, 1H, CHHC$_6$H$_5$), 4.42 (dd, J = 6.1, 15.0 Hz, 1H, NCHH), 4.05−3.90 (m, 1H, NCHH), 3.96 (s, 3H, OCH_3), 1.53 (s, 9H), 1.30 (s, 6H, two CH_3); ^{13}C NMR ($CDCl_3$, 100 MHz) δ 159.4, 154.2, 153.9, 139.6, 136.5, 135.7, 134.3, 128.6, 128.1, 127.5, 127.2, 124.2, 119.8, 118.2, 113.6, 106.3, 106.2, 80.0, 70.3, 55.4, 46.4, 28.2, 25.7, 17.6; IR (KBr) ν_{max} 2929, 1680, 1623, 1452, 1414, 1381, 1223, 1151, 1035, 972, 916, 841, 700 cm^{-1}; FABHRMS (NBA) m/e 526.1569 (M^+ + H, $C_{28}H_{32}BrNO_4$ requires 526.1593).

Anal. Calcd for $C_{28}H_{32}BrNO_4$: C, 63.88; H, 6.13; N, 2.66. Found: C, 63.66; H, 6.15; N, 2.68.

2-[*N*-(*tert*-Butyloxycarbonyl)-*N*-(formylmethyl)amino]-4-(benzyloxy)-1-bromo-7-methoxynaphthalene (23). A solution of **22** (755 mg, 1.43 mmol) in 20% CH_3OH−CH_2Cl_2 (45 mL) was cooled to −78 °C and was treated with a stream of 3% O_3/O_2 (100 L/h) for 2.9 min. The reaction was immediately quenched with the addition of 4.5 mL (61 mmol, 43 equiv) of Me_2S. The reaction mixture was stirred at −78 °C for 5 min and at 24 °C for 6 h before the solvent was removed in vacuo. Centrifugal thin-layer chromatography (SiO_2, 2 mm Chromatotron plate, 10−20% EtOAc−hexane gradient elution)

afforded **23** (580 mg, 718 mg theoretical, 81%) as a white solid: mp 170 °C dec (EtOAc−hexane, white solid); ^{1}H NMR ($CDCl_3$, 400 MHz) two amide rotamers, δ 9.70 and 9.75 (two s, 1H, CHO), 8.20 and 8.10 (two d, J = 9.2 Hz, 1H, C5-H), 7.50 (d, J = 2.4 Hz, 1H, C8-H), 7.45 (d, J = 7.6 Hz, 2H), 7.30 (m, 3H), 7.10 (dd, J = 2.4, 9.2 Hz, 1H, C6-H), 6.80 and 6.75 (two s, 1H, C3-H), 5.21−5.06 (m, 2H, OCH_2C$_6$H$_5$), 4.58 and 4.46 (two d, J = 18.8 Hz, 1H, C*H*HCHO), 3.90 (m, 1H, CH*H*CHO), 3.91 and 3.89 (two s, 3H, OCH_3), 1.50 and 1.30 (two s, 9H); ^{13}C NMR ($CDCl_3$, 100 MHz) δ major rotamer 198.1, 159.7, 154.4, 139.5, 136.3, 134.3, 128.7, 128.2, 127.8, 127.4, 124.4, 118.6, 112.7, 106.3, 105.5, 105.2, 81.3, 70.4, 59.2, 55.4, 28.2; IR (KBr) ν_{max} 2977, 2911, 2850, 2835, 1735, 1695, 1624, 1599, 1458, 1417, 1365, 1225, 1155, 1107, 1026, 839, 741 cm^{-1}; FABHRMS (NBA) *m*/*e* 499.0969 (M^+, $C_{25}H_{26}BrNO_5$ requires 499.0994).

Anal. Calcd for $C_{25}H_{26}BrNO_5$: C, 60.01; H, 5.24; N, 2.80. Found: C, 59.81; H, 5.19; N, 3.07.

2-[*N*-(*tert*-Butyloxycarbonyl)-*N*-(3-(tetrahydropyranyloxy)-2-propen-1-yl)amino]-4-(benzyloxy)-1-bromo-7-methoxynaphthalene (24). A suspension of triphenyl[(2-tetrahydropyranyloxy)methyl]phosphonium chloride[54] (371 mg, 0.90 mmol, 3.0 equiv) in 2 mL of THF at −78 °C was treated dropwise with *n*-BuLi (0.727 mL, 1.18 M in hexane, 0.86 mmol, 2.86 equiv). The reaction mixture was stirred at −78 °C for 5 min and allowed to warm to 24 °C over 10 min. The mixture was recooled to −78 °C, and **23** (154 mg, 0.30 mmol) in THF (1 mL) was added dropwise followed by HMPA (1.2 mL, 24 equiv). The reaction mixture was stirred 20 min at −78 °C and 5 h at 24 °C before the reaction was quenched with the addition of phosphate buffer (51 mL, pH 7.4). The mixture was extracted with EtOAc (3 × 20 mL), and the combined organic phase was dried (Na_2SO_4) and concentrated in vacuo. Chromatography (SiO_2, 5−30% EtOAc−hexane gradient elution containing 2% Et_3N) afforded **24** (154 mg, 175 mg theoretical, 88%) as an oil and as a mixture of *E*- and *Z*-olefin isomers: ^{1}H NMR ($CDCl_3$, 400 MHz) *E*- and *Z*-isomers and amide rotamers δ 8.10 (m, 1H, C5-H), 7.5−7.3 (m, 7H), 7.00 (m, 1H, C6-H), 6.7−6.5 (m, 1H, C*H*=CH), 6.3−6.0 (m, 1H, CH=C*H*), 5.2−5.0 (m, 2H, CH_2C$_6$H$_5$), 4.8−4.2 (m, 3H), 3.98−2.70 (m, 5H), 1.6−1.3 (m, 15H); IR (film) ν_{max} 2947, 2871, 1704, 1622, 1597, 1453, 1415, 1367, 1227, 1161, 1035, 960, 901, 841, 742, 697, 651 cm^{-1}; FABHRMS (NBA−CsI) *m*/*e* 730.0800 (M^+ + Cs, $C_{31}H_{36}BrNO_6$ requires 730.0780).

Anal. Calcd for $C_{31}H_{36}BrNO_6$: C, 62.21; H, 6.06; N, 2.34. Found: C, 62.42; H, 6.27; N, 2.45.

5-(Benzyloxy)-3-(*tert*-Butyloxycarbonyl)-8-methoxy-1-((tetrahydropyranyloxy)methyl)-1,2-dihydro-3*H*-benz[*e*]-indole (25). A solution of **24** (950 mg, 1.59 mmol) and AIBN (4.4 mg, 0.32 mmol, 0.2 equiv) in C_6H_6 (60 mL) at 24 °C under Ar was treated with Bu_3SnH (925 mg, 3.18 mmol, 2 equiv), and the reaction mixture was warmed at reflux for 2 h. The reaction mixture was cooled, and the solvent was removed in vacuo. Centrifugal thin-layer chromatography (SiO_2, 4 mm Chromatotron plate, 5−10% EtOAc−hexane gradient elution containing 2% Et_3N) afforded **25** (785 mg, 826 mg theoretical, 95%, typically 95−98%) as a pale yellow oil: ^{1}H NMR ($CDCl_3$, 400 MHz) δ 8.10 (d, J = 9.2 Hz, 1H, C6-H), 7.65 (br s, 1H, C4-H), 7.45−7.25 (m, 5H), 6.95 (d, J = 2.4 Hz, 1H, C9-H), 6.88 (dd, J = 2.4, 9.2 Hz, 1H, C7-H), 5.20 (br s, 2H, CH_2C$_6$H$_5$), 4.60 and 4.50 (two br s and m, 1H, OC*H*CH$_2$), 4.20−3.20 (m, 10H), 1.90−1.50 (m, 15H); ^{13}C NMR ($CDCl_3$, 100 MHz) δ 158.7, 155.6, 153.0, 137.0, 132.0, 128.51, 128.45, 127.9, 127.5, 125.0, 117.4, 115.0, 101.4, 100.1, 98.3, 94.6, 70.1, 68.9, 62.7, 60.4, 55.3, 52.9, 30.6, 28.5, 25.9, 19.7, 14.2; IR (film) ν_{max} 2942, 1700, 1623, 1451, 1405, 1368, 1228, 1141, 1029, 986, 907, 834, 737 cm^{-1}; FABHRMS (NBA) *m*/*e* 519.2597 (M^+ + Cs, $C_{31}H_{37}NO_6$ requires 519.2621).

5-(Benzyloxy)-3-(*tert*-butyloxycarbonyl)-1-(hydroxymethyl)-8-methoxy-1,2-dihydro-3*H*-benz[*e*]indole (26). Method A, from 25. A solution of **25** (207 mg, 0.40 mmol) in CH_3OH (6.5 mL) was treated with Amberlyst 15 (12.5 mg), and the reaction mixture was warmed at 45 °C for 6 h. The resin was removed by filtration, and the solvent was concentrated in vacuo. Chromatography (SiO_2, 20−40% EtOAc−hexane gradient elution) afforded **26** (171 mg, 172.5 mg theoretical, 99%) as a colorless solid: mp 158−160 °C (hexane, colorless solid); ^{1}H NMR ($CDCl_3$, 400 MHz) δ 8.10 (d, J = 9.6 Hz, 1H, C6-H), 7.80 (br s, 1H, C4-H), 7.51 (d, J = 7.2 Hz, 2H), 7.40 (t, J = 7.1 Hz, 2H), 7.36−7.32 (m, 1H), 6.96 (br s, 1H, C9-H), 6.95 (dd, J = 9.6, 2.5 Hz, 1H, C7-H), 5.20 (br s, 2H, CH_2C$_6$H$_5$), 4.17 (d, J = 11.0 Hz, 1H, C2-H), 4.10 (dd, J = 11.0, 8.4 Hz, 1H, C2-H), 3.93−3.90 (m, 1H, C1-H), 3.89 (s, 3H, OCH_3), 3.70 (m, 2H, CH_2OH), 1.50 (s, 9H); ^{13}C NMR ($CDCl_3$, 100 MHz) δ 158.9, 155.8, 152.7, 142.6, 136.9, 132.0, 128.5, 127.9, 125.2, 117.5, 114.9, 113.4, 101.2, 94.6, 80.7, 70.2, 64.6, 55.2, 52.4, 41.2, 28.5; IR (KBr) ν_{max} 3405, 1691, 1625, 1588, 1478, 1449, 1407, 1366, 1227, 1140, 1028 cm^{-1}; FABHRMS (NBA−CsI) *m*/*e* 568.1101 (M^+ + Cs, $C_{26}H_{29}NO_5$ requires 568.1100).

5-(Benzyloxy)-3-(*tert*-butyloxycarbonyl)-1-(chloromethyl)-8-methoxy-1,2-dihydro-3*H*-benz[*e*]indole (27). A solution of **26** (112 mg, 0.25 mmol) and Ph_3P (135 mg, 0.50 mmol, 2 equiv) in CH_2Cl_2 (0.9 mL) at 24 °C under Ar was treated with CCl_4 (0.15 mL, 1.5 mmol, 6 equiv), and the reaction mixture was stirred for 20 h at 24 °C. Chromatography (SiO_2, 10% EtOAc−hexane) afforded **27** (113 mg, 113 mg theoretical, 100%) as a white solid: mp 148−150 °C (hexane, white solid); ^{1}H NMR ($CDCl_3$, 400 MHz) δ 8.10 (d, J = 9.2 Hz, 1H, C6-H), 7.70 (br s, 1H, C4-H), 7.50 (d, J = 6.4 Hz, 2H), 7.40−7.35 (m, 3H), 6.97 (dd, J = 2.4, 9.2 Hz, 1H, C7-H), 6.86 (d, J = 2.4 Hz, 1H, C9-H), 5.20 (s, 2H, CH_2C$_6$H$_5$), 4.22 (m, 1H, C2-H), 4.10 (t, J = 9.8 Hz, 1H, C2-H), 3.92−3.86 (m, 2H, C*H*HCl, C1-H), 3.91 (s, 3H, OCH_3), 3.40 (t, J = 11.4 Hz, 1H, CH*H*Cl), 1.58 (s, 9H); ^{13}C NMR (C_6D_6, 100 MHz) δ 159.7, 156.8, 152.6, 143.2, 137.3, 132.3, 128.6, 128.1, 127.9, 126.0, 118.2, 115.4, 113.8, 101.1, 95.4, 80.6, 70.4, 54.7, 53.2, 46.4, 42.2, 28.4; IR (KBr) ν_{max} 2971, 1699, 1626, 1456, 1405, 1367, 1334, 1144, 1029, 958, 907 cm^{-1}; FABHRMS (NBA) *m*/*e* 453.1710 (M^+, $C_{26}H_{28}ClNO_4$ requires 453.1706).

Anal. Calcd for $C_{26}H_{28}ClNO_4$: C, 68.79; H, 6.22; N, 3.09. Found: C, 68.70; H, 6.51; N, 2.78.

3-(*tert*-Butyloxycarbonyl)-1-(chloromethyl)-5-hydroxy-8-methoxy-1,2-dihydro-3*H*-benz[*e*]indole (28). A mixture of **27** (80 mg, 0.17 mmol), HCO_2NH_4 (70 mg, 1.11 mmol, 6 equiv), and 10% Pd−C (80 mg) in acetone (6 mL) was warmed at reflux for 30 min. The catalyst was removed by filtration, and the solvent was evaporated under reduced pressure. Centrifugal thin-layer chromatography (SiO_2, 40% EtOAc−hexane) afforded **28** (61 mg, 64 mg theoretical, 95%, typically 95−100%) as a white solid; ^{1}H NMR ($CDCl_3$, 400 MHz) δ 8.10 (d, J = 9.2 Hz, 1H, C6-H), 7.50 (br s, 1H, C4-H), 6.95 (dd, J = 2.4, 9.2 Hz, 1H, C7-H), 6.84 (d, J = 2.4 Hz, 1H, C9-H), 6.05 (br s, 1H, OH), 4.22 (m, 1H, C2-H), 4.10 (t, J = 11.6 Hz, 1H, C2-H), 3.98−3.80 (m, 2H, C*H*HCl, C1-H), 3.91 (s, 3H, OCH_3), 3.40 (t, J = 11.4 Hz, 1H, CH*H*Cl), 1.60 (s, 9H); IR (KBr) ν_{max} 3336, 2929, 1674, 1629, 1595, 1477, 1421, 1374, 1223, 1141, 1029, 822, 713 cm^{-1}; FABHRMS (NBA−CsI) *m*/*e* 496.0287 (M^+ + Cs, $C_{19}H_{22}ClNO_4$ requires 496.0292).

Resolution of 28. The enantiomers of **28** were resolved on a HPLC semipreparative Diacel Chiralcel OD column (10 μm, 2 × 25 cm) using 2% *i*-PrOH−hexane eluant (5 mL/min). The enantiomers eluted with retention times of 48.03 (unnatural enantiomer) and 41.05 min (natural enantiomer, α = 1.17).

Natural (1*S*)-**28**: $[\alpha]^{23}_D$ −42 (*c* 0.25, CH_2Cl_2).

ent-(1*R*)-**28**: $[\alpha]^{23}_D$ +41 (*c* 0.25, CH_2Cl_2).

***N*-(*tert*-Butyloxycarbonyl)-7-methoxy-1,2,9,9a-tetrahydrocyclopropa[*c*]benz[*e*]indol-4-one (29, *N*-BOC-MCBI).** A solution of **28** (1.5 mg, 4.1 μmol) in THF−DMF (3:1, 200 μL) at 0 °C under N_2 was treated with a suspension of NaH (0.5 mg, 60% in an oil dispersion, 12 μmol, 3 equiv). The reaction mixture was allowed to stir at 0 °C for 30 min before the addition of pH 7 phosphate buffer (0.2 M, 250 μL) and 2 mL of THF. The organic layer was dried (Na_2SO_4) and concentrated in vacuo. Chromatography (SiO_2, 20−30% EtOAc−hexane gradient elution) afforded **29** (1.2 mg, 1.3 mg theoretical, 89%) as a white foam: mp 90−92 °C (hexane−EtOAc, colorless prisms); ^{1}H NMR ($CDCl_3$, 400 MHz) δ 8.10 (d, J = 8.7 Hz, 1H, C5-H), 6.90 (dd, J = 2.4, 8.7 Hz, 1H, C6-H), 6.70 (br s, 1H, C3-H), 6.25 (d, J = 2.4 Hz, 1H, C8-H), 4.10 (m, 2H, C1-H$_2$), 3.80 (s, 3H, OCH_3), 2.60 (dt, J = 4.1, 7.6 Hz,

1H, C9a-H), 1.56 (s, 9H), 1.43 (t, J = 5 Hz, 1H, C9-H), 1.23 (t, J = 7.1 Hz, 1H, C9−H); ^{13}C NMR (C_6D_6, 100 MHz) δ 184.5, 162.6, 157.9, 151.8, 142.6, 129.6, 127.4, 111.9, 109.4, 106.7, 82.4, 54.9, 52.4, 33.2, 28.6, 27.9, 23.1; IR (film) ν_{max} 2974, 1724, 1622, 1599, 1477, 1398, 1370, 1297, 1239, 1162, 1122, 1021 cm^{-1}; UV (CH_3OH) λ_{max} 312 (ϵ = 18 000), 275 nm (ϵ = 16 000); UV (THF) λ_{max} 301 (ϵ = 25 000), 270 nm (ϵ = 20 000); FABHRMS (NBA) m/e 328.1561 ($M^+ + H$, $C_{19}H_{21}NO_4$ requires 328.1549).

Natural (+)-**29**: $[\alpha]^{23}_D$ +144 (*c* 0.043, THF).

ent-(−)-**29**: $[\alpha]^{23}_D$ −142 (*c* 0.031, THF).

7-Methoxy-1,2,9,9a-tetrahydrocyclopropa[*c*]benz[*e*]indol-4-one (MCBI, 30). Phenol **28** (5 mg, 1.37 μmol) was treated with anhydrous 3 N HCl−EtOAc (0.4 mL) at 24 °C for 20 min. The solvent was removed in vacuo to afford the crude, unstable amine hydrochloride. This residue was treated with 5% aqueous $NaHCO_3$ (0.4 mL) and THF (0.4 mL) at 24 °C under N_2, and the two-phase mixture was stirred for 1.5 h (24 °C). The reaction mixture was extracted with EtOAc (3 × 2 mL), and the combined extracts were washed with H_2O (2 mL), dried (Na_2SO_4), and concentrated in vacuo. Chromatography (SiO_2, 10% CH_3OH−CH_2Cl_2) afforded **30** (2.9 mg, 3.1 mg theoretical, 93%) as a tan oil: ^{1}H NMR ($CDCl_3$, 400 MHz) δ 8.10 (d, J = 8.7 Hz, 1H, C5-H), 6.87 (dd, J = 2.4, 8.7 Hz, 1H, C6-H), 6.27 (d, J = 2.4 Hz, 1H, C8-H), 5.65 (s, 1H, C3-H), 4.80 (br s, 1H, NH), 3.80 (s, 3H, OCH_3), 3.79 (dd, J = 5.2, 10.2 Hz, 1H, C1-H), 3.63 (d, J = 10.2 Hz, 1H, C1-H), 2.78 (dt, J = 7.8, 4.6 Hz, 1H, C9a-H), 1.40 (dd, J = 4.0, 7.8 Hz, 1H, C9-H), 1.23 (t, J = 4.4 Hz, 1H, C9-H); IR (film) ν_{max} 3384, 2917, 2848, 1738, 1611, 1525, 1462, 1361, 1236, 1028 cm^{-1}; UV (CH_3OH) λ_{max} 335 (ϵ = 9400), 270 (ϵ = 10 400), 223 (ϵ = 12 500) nm; UV (THF) λ_{max} 314 (ϵ = 8200), 265 (ϵ = 8900), 224 (ϵ = 13 900) nm; FABHRMS (NBA) m/e 228.1023 ($M^+ + H$, $C_{14}H_{13}NO_2$ requires 228.1025).

Natural (+)-**30**: $[\alpha]^{23}_D$ +200 (*c* 0.04, THF).

ent-(−)-**30**: $[\alpha]^{23}_D$ −194 (*c* 0.05, THF).

A single-crystal X-ray structure determination of **30** was conducted on cubes grown from 90% EtOAc−CH_3OH, Figure 1.[69]

***N*-(*tert*-Butyloxycarbonyl)-4-(benzyloxy)-1-iodo-7-methoxy-2-naphthylamine (31).** A solution of **20** (985 mg, 2.60 mmol) in 40 mL of a 1:1 mixture of THF−CH_3OH was cooled to −78 °C, and 30 mg of TsOH−H_2O in 1 mL of THF was added. *N*-Iodosuccinimide (652 mg, 2.90 mmol) in 10 mL of THF was introduced by cannula over 5 min. Upon complete reaction (*ca.* 3 h at −78 °C), 10 mL of saturated aqueous $NaHCO_3$ and 50 mL of Et_2O were added. The reaction was warmed to 25 °C, and solid NaCl was added to saturate the aqueous layer. The organic layer was separated, and the aqueous layer was extracted with Et_2O (3 × 10 mL). The organic layers were combined, washed with saturated aqueous $NaHCO_3$ (1 × 10 mL) and saturated aqueous NaCl (2 × 10 mL), dried (Na_2SO_4), and concentrated. Chromatography (SiO_2, 2 × 4 cm, 20% EtOAc−hexane) provided **31** (1.17 g, 1.31 g, theoretical, 89%, typically 85−95%) as a crystalline white solid: mp 139−141 °C (EtOAc−hexane, needles); ^{1}H NMR ($CDCl_3$, 400 MHz) δ 8.12 (d, J = 9.1 Hz, 1H, C5-H), 7.90 (s, 1H, C3-H), 7.52 (d, J = 7.1 Hz, 2H), 7.41 (t, J = 7.6 Hz, 2H), 7.36 (d, J = 2.4 Hz, 1H, C8-H), 7.34 (t, J = 7.4 Hz, 1H), 7.28 (br s, 1H, NH), 6.99 (dd, J = 9.1, 2.4 Hz, 1H, C6-H), 5.24 (s, 2H, OCH_2Ph), 3.95 (s, 3H, OCH_3), 1.56 (s, 9H); ^{13}C NMR ($CDCl_3$, 100 MHz) δ 160.1, 155.8, 152.7, 138.9, 136.6, 136.4, 128.5, 128.0, 127.8, 124.6, 118.5, 116.3, 110.8, 98.1, 81.1, 79.4, 70.3, 55.3, 28.3; IR (film) ν_{max} 3387, 2978, 2923, 1730, 1621, 1602, 1572, 1503, 1366, 1230, 1152 cm^{-1}; FABHRMS (NBA−CsI) m/e 637.9836 (M^+ + Cs, $C_{23}H_{24}INO_4$ requires 637.9804).

Anal. Calcd for $C_{23}H_{24}INO_4$: C, 54.67; H, 4.79; N, 2.77. Found: C, 54.61; H, 4.85, N. 2.92.

2-[*N*-(*tert*-Butyloxycarbonyl)-*N*-(2-propenyl)amino]-4-(benzyloxy)-1-iodo-7-methoxy-2-naphthylamine (32). A solution of **31** (820 mg, 1.62 mmol) in 25 mL of DMF cooled to 0 °C was treated with NaH (80 mg, 60% in oil, 2.0 mmol) in several portions over 10 min. After 45 min, allyl bromide (605 mg, 5 mmol) was added and the reaction mixture was allowed to warm to 25 °C and stirred for 3 h. The reaction was quenched by addition of saturated aqueous $NaHCO_3$ (15 mL), and the aqueous layer was extracted with EtOAc (4 × 15 mL). The organic layers were combined, washed with H_2O (2 × 10 mL) and saturated aqueous NaCl (2 × 10 mL), dried (Na_2SO_4), filtered, and concentrated under reduced pressure. Centrifugal thin-layer chromatography (SiO_2, 4 mm Chromatotron plate, 5−15% EtOAc−hexane gradient elution) provided **32** (822 mg, 884 mg theoretical, 93%, typically 90−95%) as a crystalline white solid (mixture of amide rotamers in $CDCl_3$): mp 112−113 °C (EtOAc−hexane); ^{1}H NMR ($CDCl_3$, 400 MHz) major rotamer δ 8.21 (d, J = 9.1 Hz, 1H, C5-H), 7.53 (s, 1H, C8-H), 7.46 (d, J = 7.2 Hz, 2H), 7.39 (t, J = 7.0 Hz, 2H), 7.33 (t, J = 7.2 Hz, 1H), 7.13 (dd, J = 9.1, 1.8 Hz, 1H, C6-H), 6.60 (s, 1H, C3-H), 5.97−5.87 (m, 1H, C*H*=CH_2), 5.28−4.98 (m, 4H), 4.51 (dd, J = 15.0, 5.9 Hz, 1H, NC*H*H), 3.97 (s, 3H, OCH_3), 3.81 (dd, J = 15.0, 7.2 Hz, 1H, NCH*H*), 1.30 (s, 9H); ^{13}C NMR ($CDCl_3$, 100 MHz) δ 159.9, 155.1, 153.9, 143.6, 137.0, 136.5, 133.6, 128.6, 128.1, 127.2, 124.4, 120.2, 118.3, 117.9, 111.9, 106.3, 93.9, 80.3, 70.2, 55.4, 52.2, 28.3; IR (film) 3077, 2976, 2923, 1703, 1621, 1594, 1450, 1410, 1367, 1324, 1263, 1226, 1149, 1030 cm^{-1}; FABHRMS (NBA−CsI) m/e 678.0089 (M^+ + Cs, $C_{26}H_{28}INO_4$ requires 678.0017).

Anal. Calcd for $C_{26}H_{28}INO_4$: C, 57.26; H, 5.17; N, 2.57. Found: 57.16; H, 5.25; N, 2.54.

5-(Benzyloxy)-3-(*tert*-butyloxycarbonyl)-8-methoxy-1-[(2′,2′,6′,6′-tetramethylpiperidinyl-*N*-oxy)methyl]-1,2-dihydro-3*H*-benz[*e*]indole (33). A solution of **32** (720 mg, 1.32 mmol) and Tempo (619 mg, 3.96 mmol) in 45 mL of freshly distilled benzene under N_2 was treated with Bu_3SnH (384 mg, 1.32 mmol). The solution was warmed at 70 °C, and three additional equivalents of Tempo (3 × 206 mg) and Bu_3SnH (4 × 384 mg) were added sequentially in four portions over the next 45 min. After 1 h, the solution was cooled to 25 °C and the volatiles were removed under reduced pressure. Centrifugal thin-layer chromatography (SiO_2, 4 mm Chromatotron plate, 0−10% EtOAc−hexanes gradient elution) provided **33** (622 mg, 758 mg theoretical, 82%, typically 75−90%) as a white solid: mp 128−130 °C (hexane, white needles); ^{1}H NMR (DMSO-d_6, 400 MHz) δ 8.01 (d, J = 9.2 Hz, 1H, C6-H), 7.62 (br s, 1H, C4-H), 7.52 (br s, 2H), 7.42 (t, J = 7.2 Hz, 2H), 7.35 (t, J = 7.3 Hz, 1H), 7.01 (d, J = 2.4 Hz, 1H, C9-H), 6.95 (dd, J = 9.2, 2.4 Hz, 1H, C7-H), 5.23 (s, 2H, OCH_2Ph), 4.16 (d, J = 11.0 Hz, 1H, C2-H), 4.01 (t, J = 11.0 Hz, 1H, C2-H), 3.92 (dd, J = 8.1, 4.6 Hz, 1H, C*H*HOR), 3.82 (s, 3H, OCH_3), 3.79−3.70 (m, 2H, CH*H*OR and C1-H), 1.51 (s, 9H), 1.46−1.19 (m, 6H), 1.14 (s, 3H, CH_3), 1.02 (s, 3H, CH_3), 0.91 (s, 3H, CH_3), 0.82 (s, 3H, CH_3); ^{13}C NMR (DMSO-d_6, 100 MHz) δ 158.7, 155.5, 152.7, 141.5, 137.0, 131.9, 128.5, 127.9, 127.5, 125.0, 117.4, 115.3, 112.8, 100.9, 94.6, 80.4, 70.1, 59.8, 59.7, 55.0, 52.8, 39.6, 39.5, 38.4, 33.2, 32.9, 31.2, 28.5, 20.14, 20.52, 17.0; IR (film) ν_{max} 2974, 2923, 1697, 1620, 1584, 1471, 1446, 1400, 1359, 1323, 1220, 1169, 1133, 1031 cm^{-1}; FABHRMS (NBA−NaI) m/e 597.3288 (M^+ + Na, $C_{35}H_{46}N_2O_5$ requires 597.3304).

Anal. Calcd for $C_{35}H_{46}N_2O_5$: C, 73.13; H, 8.07; N, 4.88. Found: C, 73.30; H, 7.94; N, 4.85.

3-(*tert*-Butyloxycarbonyl)-1-(hydroxymethyl)-5-hydroxy-8-methoxy-1,2-dihydro-3*H*-benz[*e*]indole (26). Method B, from 33. A solution of **33** (750 mg, 1.30 mmol) in 30 mL of a 3:1:1 mixture of HOAc−THF−H_2O was treated with zinc powder (1.05 g, 16 mmol), and the resulting suspension was warmed at 70 °C with vigorous stirring. After 2 h, the reaction mixture was cooled to 25 °C and the zinc was removed by filtration. The volatiles were removed under reduced pressure, and the resulting residue was dissolved in 30 mL of EtOAc and filtered. The solution was concentrated and subjected to centrifugal thin-layer chromatography (SiO_2, 4 mm Chromatotron plate, 15−35% EtOAc−hexane gradient elution) to provide **28** (487 mg, 566 mg theoretical, 86%, typically 80−90%) as a white solid identical in all respects to authentic material.

(69) The author has deposited the atomic coordinates for this structure with the Cambridge Crystallographic Data Centre. The coordinates can be obtained, upon request, from the Director, Cambridge Crystallographic Data Centre, 12 Union Road, Cambridge, CB2 1EZ, UK.

***seco*-MCBI−TMI (39).** A solution of **28** (3.5 mg, 9.6 μmol) in 4 M HCl−EtOAc (300 μL) at 0 °C was stirred for 30 min before the volatiles were removed by a stream of N_2 and the residue was dried under vacuum (0.02 mm) for 15 min. The resulting crude **34** was dissolved in DMF (200 μL) and treated sequentially with **35**[5] (2.7 mg, 10.6 μmol) and EDCI (5.5 mg, 29 μmol, 3 equiv), and the reaction mixture was stirred for 10 h at 25 °C. Water (0.5 mL) was added to the reaction mixture, and the aqueous phase was extracted with EtOAc (4 × 1 mL). The organic layers were combined, dried (Na_2SO_4), and concentrated in vacuo. Preparative thin-layer chromatography (SiO_2, 20 cm × 20 cm × 0.25 mm, 5% DMF−toluene, R_f = 0.60) afforded **39** (4.1 mg, 4.8 mg theoretical, 85%) as a white solid: ^{1}H NMR (DMSO-d_6, 400 MHz) δ 11.48 (d, J = 2.0 Hz, 1H, NH), 10.35 (s, 1H, OH), 8.02 (d, J = 9.2 Hz, 1H, C6-H), 7.74 (br s, 1H, C4-H), 7.12 (d, J = 2.4 Hz, 1H, C9-H), 7.08 (d, J = 2.0 Hz, 1H, C3′-H), 7.00 (d, J = 9.2, 2.4 Hz, 1H, C7-H), 6.98 (s, 1H, C4′-H), 4.72 (t, J = 10.5 Hz, 1H, C2-H), 4.47 (dd, J = 11.1, 1.3 Hz, 1H, C2-H), 4.19−4.15 (m, 1H, C1-H), 4.05 (dd, J = 11.3, 3.3 Hz, 1H, C*H*HCl), 3.95 (s, 3H, OCH_3), 3.93 (s, 3H, OCH_3), 3.84 (s, 3H, OCH_3), 3.82 (s, 3H, OCH_3), 3.80 (dd, J = 10.4, 5.5 Hz, 1H, CH*H*Cl); IR (film) ν_{max} 3238, 2946, 1631, 1585, 1522, 1493, 1463, 1388, 1313, 1220 cm^{-1}; FABHRMS (NBA) m/e 497.1500 (M^+ + H, $C_{26}H_{25}ClN_2O_6$ requires 497.1479).

Natural (1*S*)-**39**: $[\alpha]^{23}_D$ −23 (*c* 0.07, DMF).

ent-(1*R*)-**39**: $[\alpha]^{23}_D$ +23 (*c* 0.10, DMF).

MCBI−TMI (40). A solution of **39** (3.5 mg, 7.04 μmol) in THF−DMF (3:1, 350 μL) at 0 °C was treated with NaH (0.85 mg, 60% in oil, 21 μmol, 3 equiv). The reaction mixture was stirred for 30 min at 0 °C before the addition of pH 7 phosphate buffer (0.2 M, 400 μL) and 3 mL of THF. The organic solution was dried (Na_2SO_4) and concentrated in vacuo, and the crude product was purified by preparative thin-layer chromatography (SiO_2, 20 cm × 20 cm × 0.25 mm, 5% DMF−toluene, R_f = 0.55) to provide **40** (2.9 mg, 3.2 mg theoretical, 90%) as a white solid: ^{1}H NMR (DMSO-d_6, 400 MHz) δ 11.60 (s, 1H, NH), 7.91 (d, J = 8.8 Hz, 1H, C5-H), 7.08 (d, J = 2.0 Hz, 1H, C3′-H), 6.97 (dd, J = 8.7, 2.4 Hz, 1H, C6-H), 6.92 (s, 1H, C4′-H), 6.70 (d, J = 2.4 Hz, 1H, C8-H), 6.60 (s, 1H, C3-H), 4.50 (dd, J = 10.5, 5.0 Hz, 1H, C1-H), 4.32 (d, J = 10.5 Hz, 1H, C1-H), 3.90 (s, 3H, OCH_3), 3.84 (s, 3H, OCH_3), 3.80 (s, 3H, OCH_3), 3.79 (s, 3H, OCH_3), 3.32−3.28 (m, 1H, C9a-H, partially obscured by H_2O), 1.78 (dd, J = 7.7, 4.0 Hz, 1H, C9-H), 1.69 (t, J = 4.3 Hz, 1H, C9-H); IR (film) ν_{max} 2937, 1646, 1626, 1595, 1533, 1518, 1467, 1446, 1394, 1302, 1270, 1232, 1108 cm^{-1}; FABHRMS (NBA) m/e 461.1732 (M^+ + H, $C_{26}H_{24}N_2O_6$ requires 461.1713).

Natural (+)-**40**: $[\alpha]^{23}_D$ +204 (*c* 0.05, THF).

ent-(−)-**40**: $[\alpha]^{23}_D$ −206 (*c* 0.05, THF).

***seco*-MCBI−Indole$_2$ (41).** A solution of **28** (4.3 mg, 11.8 μmol) in 4 M HCl−EtOAc (350 μL) at 0 °C was stirred for 30 min before the volatiles were removed by a stream of N_2 and the residue was dried under vacuum (0.02 mm) for 15 min. The resulting crude **34** was dissolved in DMF (250 μL) and treated sequentially with **36**[40] (4.2 mg, 13.0 μmol) and EDCI (6.8 mg, 35 μmol, 3 equiv), and the mixture was stirred for 10 h at 25 °C. Water (0.5 mL) was added to the reaction mixture, and the aqueous phase was extracted with EtOAc (4 × 1 mL). The organic layers were combined, dried (Na_2SO_4), and concentrated in vacuo. Preparative thin-layer chromatography (20 cm × 20 cm × 0.25 mm, 15% DMF−toluene, R_f = 0.45) afforded **41** (5.2 mg, 6.7 mg theoretical, 78%) as a tan solid: ^{1}H NMR (DMSO-d_6, 400 MHz) δ 11.72 (s, 2H, NH), 10.32 (s, 1H, OH), 10.16 (s, 1H, NH), 8.22 (s, 1H, C4′-H), 8.02 (d, J = 9.2 Hz, 1H, C6-H), 7.82 (br s, 1H, C4-H), 7.67 (d, J = 8.2 Hz, 1H, C4″-H), 7.58 (dd, J = 8.9, 1.8 Hz, 1H, C6′-H), 7.49 (d, J = 8.4 Hz, 1H, C7″-H), 7.47 (d, J = 7.8 Hz, 1H, C7′-H), 7.42 (s, 1H, C3′ or C3″-H), 7.23 (s, 1H, C3′ or C3″-H), 7.21 (t, J = 8.1 Hz, 1H, C6″-H), 7.12 (d, J = 2.2 Hz, 1H, C9-H), 7.06 (t, J = 7.2 Hz, 1H, C5″-H), 6.98 (dd, J = 9.2, 2.4 Hz, 1H, C7−H), 4.79 (t, J = 10.4 Hz, 1H, C2-H), 4.57 (d, J = 10.1 Hz, 1H, C2-H), 4.25−4.21 (m, 1H, C1-H), 4.04 (dd, J = 11.0, 3.0 Hz, 1H, C*H*HCl), 3.86 (dd, J = 11.0, 6.3 Hz, 1H, CH*H*Cl), 3.91 (s, 3H, OCH_3); IR (film) ν_{max} 3280, 2920, 1693, 1647, 1630, 1589, 1518, 1455, 1417, 1308, 1220 cm^{-1}; FABHRMS (NBA−CsI) m/e 565.1655 (M^+ + H, $C_{32}H_{25}ClN_4O_4$ requires 565.1643).

Natural (1*S*)-**41**: $[\alpha]^{23}_D$ +54 (*c* 0.08, DMF).

ent-(1*R*)-**41**: $[\alpha]^{23}_D$ −55 (*c* 0.07, DMF).

MCBI−Indole$_2$ (42). A solution of **41** (2.8 mg, 4.95 μmol) in THF−DMF (3:1, 250 μL) at 0 °C was treated with NaH (0.59 mg, 60% in oil, 15 μmol, 3 equiv), and the mixture was stirred for 30 min at 0 °C. The reaction was quenched with the addition of pH 7 phosphate buffer (0.2 M, 250 μL) and 3 mL of THF. The organic solution was dried (Na_2SO_4), concentrated in vacuo, and purified by preparative thin-layer chromatography (20 cm × 20 cm × 0.25 mm, 15% DMF−toluene, R_f = 0.40) to provide **42** (2.25 mg, 2.62 mg theoretical, 86%) as a tan solid: ^{1}H NMR (DMSO-d_6, 400 MHz) δ 11.82 (s, 1H, NH), 11.70 (s, 1H, NH), 10.17 (s, 1H, NH), 8.21 (s, 1H, C4′-H), 7.94 (d, J = 8.7 Hz, 1H, C5-H), 7.66 (d, J = 8.0 Hz, 1H, C4″-H), 7.59 (dd, J = 8.8, 1.7 Hz, 1H, C6′-H), 7.47 (apparent d, J = 9.2 Hz, 2H, C7′-H and C7″-H), 7.41 (s, 1H, C3′ or C3″-H), 7.27 (d, J = 1.6 Hz, 1H, C3′ or C3″-H), 7.21 (t, J = 7.2 Hz, 1H, C6″-H), 7.06 (t, J = 7.2 Hz, 1H, C5″-H), 6.98 (dd, J = 8.7, 2.3 Hz, 1H, C6-H), 6.89 (s, 1H, C3-H), 6.72 (d, J = 2.3 Hz, 1H, C8-H), 4.62 (dd, J = 10.3, 5.0 Hz, 1H, C1-H), 4.49 (d, J = 10.3 Hz, 1H, C1-H), 3.92−3.87 (m, 1H, C9a-H), 3.85 (s, 3H, OCH_3), 1.77 (dd, J = 7.7, 4.0 Hz, 1H, C9-H), 1.67 (d, J = 4.0 Hz, 1H, C9-H); IR (film) ν_{max} 2944, 1647, 1586, 1550, 1517, 1391, 1234, 1137, 1067, 1025 cm^{-1}; FABHRMS (NBA) m/e 529.1889 (M^+ + H, $C_{32}H_{24}N_4O_4$ requires 529.1876).

Natural (+)-**42**: $[\alpha]^{23}_D$ +122 (*c* 0.04, DMF).

ent-(−)-**42**: $[\alpha]^{23}_D$ −120 (*c* 0.07, DMF).

***seco*-MCBI−CDPI$_1$ (43).** A solution of **28** (3.9 mg, 10.7 μmol) in 4 M HCl−EtOAc (300 μL) at 0 °C was stirred for 30 min before the volatiles were removed by a stream of N_2 and the residue was dried under vacuum (0.02 mm) for 15 in. The resulting crude **34** was dissolved in DMF (200 μL) and treated sequentially with **37**[59] (2.9 mg, 11.8 μmol) and EDCI (6.1 mg, 32 μmol, 3 equiv), and the mixture was stirred at 25 °C for 12 h. Water (0.5 mL) was added to the reaction mixture, and the aqueous phase was extracted with EtOAc (4 × 1 mL). The organic layers were combined, dried (Na_2SO_4), and concentrated in vacuo. Preparative thin-layer chromatography (20 cm × 20 cm × 0.25 mm, 30% DMF−toluene, R_f = 0.65) afforded **43** (3.7 mg, 5.2 mg theoretical, 71%) as a light yellow solid: ^{1}H NMR (DMSO-d_6, 400 MHz) δ 11.60 (d, J = 2.0 Hz, 1H, NH), 10.31 (s, 1H, OH), 8.01 (d, J = 9.2 Hz, 1H, C6-H), 7.99 (d, J = 8.9 Hz, 1H, C4′-H), 7.80 (br s, 1H, C4-H), 7.23 (d, J = 8.9 Hz, 1H, C5′-H), 7.10 (d, J = 2.4 Hz, 1H, C9-H), 7.00 (d, J = 1.5 Hz, 1H, C8′-H), 6.98 (dd, J = 9.2, 2.4 Hz, 1H, C7-H), 6.10 (br s, 2H, NH_2), 4.77 (t, J = 10.8 Hz, 1H, C2-H), 4.54 (dd, J = 11.0, 1.4 Hz, 1H, C2-H), 4.22−4.17 (m, 1H, C1-H), 4.04 (dd, J = 11.1, 3.1 Hz, 1H, C*H*HCl), 3.98 (t, J = 8.8 Hz, 2H, C2′-H_2), 3.92 (s, 3H, OCH_3), 3.86 (dd, J = 11.1, 7.2 Hz, 1H, CH*H*Cl), 3.25 (t, J = 8.8 Hz, 2H, C1′-H_2 partially obscured by H_2O); IR (film) ν_{max} 3292, 2923, 1659, 1630, 1595, 1504, 1446, 1415, 1384, 1224 cm^{-1}; FABHRMS (NBA) m/e 490.1411 (M^+, $C_{26}H_{23}ClN_4O_4$ requires 490.1408).

Natural (1*S*)-**43**: $[\alpha]^{23}_D$ +74 (*c* 0.09, DMF).

ent-(1*R*)-**43**: $[\alpha]^{23}_D$ −76 (*c* 0.11, DMF).

MCBI−CDPI$_1$ (44). A solution of **43** (1.8 mg, 3.67 μmol) in THF−DMF (3:1, 200 μL) at 0 °C was treated with NaH (0.44 mg, 60% in oil, 11 μmol, 3 equiv). The mixture was stirred at 0 °C for 30 min before the reaction was quenched with the addition of pH 7 phosphate buffer (0.2 M, 200 μL) and 3 mL of THF. The organic solution was dried (Na_2SO_4), concentrated in vacuo, and purified by preparative thin-layer chromatography (20 cm × 20 cm × 0.25 mm, 30% DMF−toluene, R_f = 0.65) to provide **44** (1.50 mg, 1.67 mg theoretical, 90%) as a light yellow solid: ^{1}H NMR (DMSO-d_6, 400 MHz) δ 11.70 (s, 1H, NH), 8.01 (d, J = 9.2 Hz, 1H, C4′-H), 7.93 (d, J = 8.4 Hz, 1H, C5-H), 7.21 (d, J = 8.8 Hz, 1H, C5′-H), 7.06 (s, 1H, C8′-H), 6.98 (dd, J = 8.6, 2.2 Hz, 1H, C6-H), 6.86 (s, 1H, C3-H), 6.71 (d, J = 2.2 Hz, 1H, C8-H), 6.11 (br s, 2H, NH_2), 4.58 (dd, J = 10.3, 4.9 Hz, 1H, C1-H), 4.46 (d, J = 10.3 Hz, 1H, C1-H), 3.97 (t, J = 8.5 Hz, 2H, C2′-H_2), 3.85 (s, 3H, OCH_3), 3.38−3.30 (m, 3H, C9a, C1′-H_2 partially obscured by H_2O), 1.77 (dd, J = 7.8, 4.1 Hz, 1H, C9-H), 1.66 (t, J = 4.1 Hz, 1H, C9-H); IR (film) ν_{max} 3375, 2937, 1652, 1597, 1572, 1501, 1455, 1426, 1388, 1359, 1334, 1300, 1267, 1229, cm^{-1}; FABHRMS (NBA) m/e 455.1730 (M^+ + H, $C_{26}H_{22}N_4O_4$ requires 455.1719).

Natural (+)-**44** $[\alpha]^{23}_D$ +183 (*c* 0.07, DMF).

ent-(−)-**44**: $[\alpha]^{23}_D$ −187 (*c* 0.08, DMF).

***seco*-MCBI−CDPI$_2$ (45).** A solution of **28** (3.6 mg, 9.8 μmol) in 4 M HCl−EtOAc (300 μL) at 0 °C was stirred for 30 min before the volatiles were removed by a stream of N_2 and the residue was dried under vacuum (0.02 mm) for 15 min. The resulting crude **34** was dissolved in DMF (200 μL) and treated sequentially with **38**[59] (4.6 mg, 10.7 μmol) and EDCI (5.6 mg, 29 μmol, 3 equiv), and the mixture was stirred for 6 h at 25 °C. The solvent was removed under vacuum, water (0.5 mL) was added to the mixture, and the insoluble crude product was collected by centrifugation. Preparative thin-layer chromatography (20 cm × 20 cm × 0.25 mm, 33% DMF−toluene, R_f = 0.50) afforded **43** (4.5 mg, 6.6 mg theoretical, 68%) as a light yellow solid: ^{1}H NMR (DMSO-d_6, 400 MHz) δ 11.80 (d, *J* = 1.6 Hz, 1H, NH), 11.55 (d, *J* = 1.2 Hz, 1H, NH), 10.31 (s, 1H, OH), 8.28 (d, *J* = 7.0 Hz, 1H, C4′-H), 8.01 (d, *J* = 9.2 Hz, 1H, C6-H), 7.97 (d, *J* = 8.9 Hz, 1H, C4″-H), 7.82 (br s, 1H, C4-H), 7.38 (d, *J* = 9.0 Hz, 1H, C5″-H), 7.22 (d, *J* = 8.8 Hz, 1H, C5′-H), 7.16 (d, *J* = 1.3 Hz, 1H, C8″-H), 7.12 (d, *J* = 2.3 Hz, 1H, C9-H), 6.98 (dd, *J* = 9.2, 2.4 Hz, 1H, C7-H), 6.97 (s, 1H, C8′-H), 6.10 (br s, 2H, NH_2), 4.80 (t, *J* = 10.8 Hz, 1H, C2-H), 4.66 (t, *J* = 8.3 Hz, 2H, C2′-H_2), 4.57 (d, *J* = 11.0 Hz, 1H, C2-H), 4.23−4.21 (m, 1H, C1-H), 4.05 (dd, *J* = 11.0, 3.0 Hz, 1H, C*H*HCl), 3.96 (t, *J* = 8.8 Hz, 2H, C2″-H_2), 3.91 (s, 3H, OCH_3), 3.87 (dd, *J* = 11.0, 4.2 Hz, 1H, CH*H*Cl), 3.52−3.35 (m, 4H, C1′-H_2, C1″-H_2 partially obscured by H_2O); IR (film) ν_{max} 3374, 2913, 2851, 1662, 1651, 1605, 1446, 1425, 1359, 1282, 1241, 1164 cm^{-1}; FABHRMS (NBA) *m*/*e* 675.2143 (M^+ + H, $C_{37}H_{31}ClN_6O_5$ requires 675.2123).

Natural (1*S*)-**45**: $[\alpha]^{23}_D$ +50 (*c* 0.05, DMF).

ent-(1*R*)-**45**: $[\alpha]^{23}_D$ −52 (*c* 0.04, DMF).

MCBI−CDPI$_2$ (46). A solution of **45** (0.57 mg, 0.84 μmol) in THF−DMF (3:1, 50 μL) at 0 °C was treated with NaH (0.10 mg, 2.5 μmol, 3 equiv), and the mixture was stirred at 0 °C for 30 min. The reaction was quenched with the addition of pH 7 phosphate buffer (0.2 M, 50 μL) and 2 mL of THF. The organic solution was dried (Na_2SO_4), concentrated in vacuo, and purified by preparative thin-layer chromatography (5 cm × 20 cm × 0.25 mm, 33% DMF−toluene, R_f = 0.45) to provide **46** (0.51 mg, 0.54 mg theoretical, 94%) as a light yellow solid: ^{1}H NMR (DMSO-d_6, 400 MHz) δ 11.90 (d, *J* = 2.0 Hz, 1H, NH), 11.55 (d, *J* = 2.0 Hz, 1H, NH), 8.29 (d, *J* = 8.1 Hz, 1H, C4′-H), 7.97 (d, *J* = 8.9 Hz, 1H, C4″-H), 7.93 (d, *J* = 8.8 Hz, 1H, C5-H), 7.36 (d, *J* = 8.9 Hz, 1H, C5″-H), 7.22 (d, *J* = 1.7 Hz, 1H, C8″-H), 7.21 (d, *J* = 8.7 Hz, 1H, C5′-H), 6.98 (dd, *J* = 8.8, 2.4 Hz, 1H, C7-H), 6.96 (d, *J* = 1.3 Hz, 1H, C8′-H), 6.88 (s, 1H, C3-H), 6.73 (d, *J* = 2.4 Hz, 1H, C8-H), 6.10 (br s, 2H, NH_2), 4.65 (t, *J* = 8.2 Hz, 2H, C2′-H_2), 4.61 (dd, *J* = 10.5, 4.8 Hz, 1H, C1-H), 4.50 (d, *J* = 10.5 Hz, 1H, C1-H), 3.98 (t, *J* = 8.7 Hz, 2H, C2″-H_2), 3.86 (s, 3H, OCH_3), 3.50−3.35 (m, 5H, C1′-H_2, C1″-H_2, C9a-H partially obscured by H_2O), 1.78 (dd, *J* = 7.8, 4.0 Hz, 1H, C9-H), 1.68 (t, *J* = 4.3 Hz, 1H, C9-H); IR (film) ν_{max} 3372, 2920, 1656, 1602, 1581, 1501, 1430, 1392, 1363, 1338, 1267, 1229, 1141, 1019 cm^{-1}; FABHRMS (NBA−CsI) *m*/*e* 771.1244 (M^+ + Cs, $C_{37}H_{30}N_6O_5$ requires 771.1332).

Natural (+)-**46**: $[\alpha]^{23}_D$ +145 (*c* 0.01, DMF).

ent-(−)-**46**: $[\alpha]^{23}_D$ −149 (*c* 0.01, DMF).

Solvolysis Reactivity. pH 3. *N*-BOC-MCBI (**29**, 0.1 mg) was dissolved in CH_3OH (1.5 mL) and mixed with pH 3 aqueous buffer (1.5 mL). The buffer contained 4:1:20 (v:v:v) 0.1 M citric acid, 0.2 M Na_2HPO_4, and H_2O, respectively. The solvolysis solution was sealed and kept at 25 °C protected from light. The UV spectrum was measured at regular intervals every 2 h during the first day, every 12 h for another week, and every 24 h for an additional week. The decrease in the long-wavelength absorption at 324 nm and the increase in the short-wavelength absorption at 266 nm were monitored, Figure 7. The solvolysis rate constant ($k = 1.75 \times 10^{-6}$ s^{-1}) and half-life ($t_{1/2}$ = 110 h) were calculated from data recorded at the short wavelength from the least-squares treatment (r = 1.0) of the slope of the plot of time versus $\ln[(A_f - A_i)/(A_f - A)]$.

Similarly, MCBI (**30**, 0.1 mg) was dissolved in CH_3OH (1.5 mL) and mixed with pH 3 aqueous buffer (1.5 mL). The solvolysis solution was sealed and stirred at 25 °C in the dark. The UV spectrum was recorded every 24 h for 2 months. The decrease in the long-wavelength absorption at 340 nm and the increase in absorption at 268 nm were monitored, Figure 7. The solvolysis rate constant ($k = 5.76 \times 10^{-7}$ s^{-1}) and half-life ($t_{1/2}$ = 334 h) were determined as detailed above (r = 0.98).

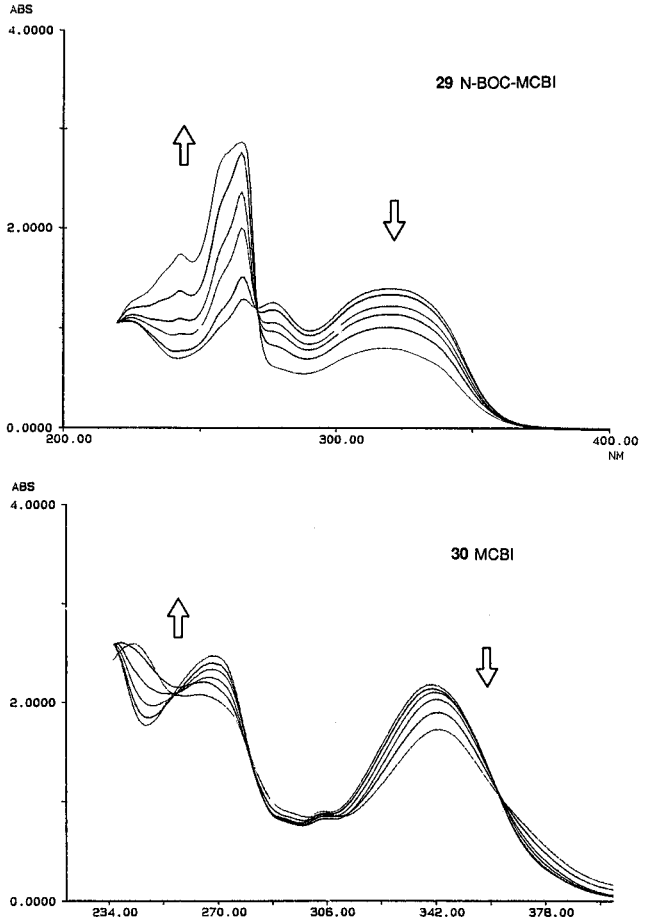

Figure 7. Solvolysis study (UV spectra) of *N*-BOC-MCBI (**29**, top) and MCBI (**30**, bottom) in 50% CH_3OH−aqueous buffer (pH 3.0, 4:1:20 (v/v/v) 0.1 M citric acid, 0.2 M Na_2HPO_4, and H_2O, respectively). The spectra were recorded at regular intervals and only a few are shown for clarity. Top: 1, 0 h; 2, 4 h; 3, 27 h; 4, 70 h; 5, 105 h; 6, 177 h. Bottom: 1, 0 h; 2, 4 h; 3, 27 h; 4, 70 h; 5, 177 h; 6, 752 h.

pH 2. Samples of **4** and **29** (50 μg) were dissolved in CH_3OH (1.5 mL), and the solutions were mixed with aqueous buffer (pH 2.05, 1.5 mL). The buffer contained 4:1:20 (v:v:v) 1.0 M citric acid, 0.2 M Na_2HPO_4, and H_2O, respectively. Immediately after mixing, the UV spectra of the solutions were measured against a reference solution containing CH_3OH (1.5 mL), and the aqueous buffer (1.5 mL) and these readings were used for the initial absorbance values. The solutions were stoppered, protected from the light, and allowed to stand at 25 °C. UV spectra were recorded at regular intervals until constant values were obtained for the long- and short-wavelength absorbances (311 and 255 nm for **4**, 322 and 265 nm for **29**). The solvolysis rate constants were determined from the slope of the lines obtained from linear least-squares treatment of plots of $\ln[(A_f - A_i)/(A_f - A)]$ versus time using the short-wavelength measurements (Figure 8). The first-order rate constants determined under these conditions were 1.53×10^{-5} s^{-1} (5.54×10^{-2} h^{-1}, $t_{1/2}$ = 12.5 h, r = 0.999) for *N*-BOC-CBI (**4**) and 1.62×10^{-5} s^{-1} (5.86×10^{-2} h^{-1}, $t_{1/2}$ = 11.8 h, r = 0.996) for *N*-BOC-MCBI (**29**).

Solvolysis Regioselectivity: 3-(*tert*-Butyloxycarbonyl)-5-hydroxy-8-methoxy-1-(methoxymethyl)-1,2-dihydro-3*H*-benz[*e*]indole (47). A solution of **29** (10.1 mg, 30.8 μmol) in 2.5 mL of CH_3OH was cooled to 0 °C, and CF_3SO_3H−CH_3OH (185 μL, 0.02 M, 0.12 equiv) was added. After 3 h, the reaction was quenched by the addition of $NaHCO_3$ (10 mg),

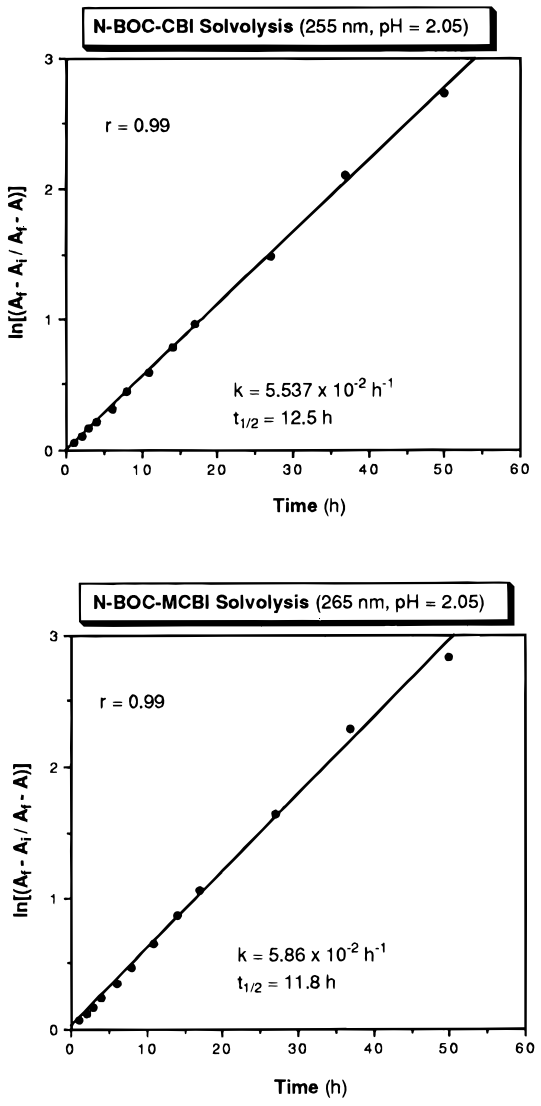

Figure 8.

the mixture was warmed to 25 °C and filtered, and the solution was concentrated. Centrifugal thin-layer chromatography (SiO_2, 0.3 mm Chromatotron plate, 30% EtOAc−hexane) provided **47** (10.5 mg, 11.1 mg theoretical, 95%) as a white solid: mp 157−159 °C (hexane, white prisms); ^{1}H NMR (C_6D_6, 400 MHz) δ 8.46 (d, J = 8.3 Hz, 1H, C6-H), 8.15 (br s, 1H, C4-H), 7.06 (dd, J = 9.2, 2.4 Hz, 1H, C7-H), 6.99 (d, J = 2.4 Hz, 1H, C9-H), 6.95 (br s, 1H, OH), 4.22 (d, J = 10.6 Hz, 1H, C2-H), 3.85−3.80 (m, 1H, C2-H), 3.66−3.63 (m, 1H, C*H*HOCH$_3$), 3.55 (dd, J = 9.2, 3.7 Hz, 1H, CH*H*OCH$_3$), 3.41 (s, 3H, OCH$_3$), 3.01−2.95 (m, 1H, C1-H), 2.97 (s, 3H, OCH$_3$), 1.44 (s, 9H); ^{13}C NMR (C_6D_6, 100 MHz) δ 159.4, 154.5, 153.4, 142.4, 132.9, 125.9, 117.5, 115.1, 114.4, 102.0, 98.0, 80.8, 74.7, 58.5, 54.7, 53.3, 37.8, 28.4; IR (film) ν_{max} 3329, 2974, 2932, 1697, 1674, 1629, 1590, 1476, 1418, 1368, 1331, 1224, 1141, 1028 cm^{-1}; FABHRMS (NBA−NaI) m/e 359.1720 (M^+, $C_{20}H_{25}NO_5$ requires 359.1733).

DNA Alkylation Studies: Selectivity and Efficiency. General procedures, the preparation of singly ^{32}P 5′ end-labeled double-stranded DNA, the agent binding studies, gel electrophoresis, and autoradiography were conducted according to procedures described in full detail elsewhere.[10] Eppendorf tubes containing the 5′ end-labeled DNA (9 μL) in TE buffer (10 mM Tris, 1 mM EDTA, pH 7.5) were treated with the agent in DMSO (1 μL at the specified concentration). The solution was mixed by vortexing and brief centrifugation and subsequently incubated at 4 or 25 °C for 24 h (natural enantiomers) or 37 °C (unnatural enantiomers) for 72 h. The covalently modified DNA was separated from unbound agent by EtOH precipitation and resuspended in TE buffer (10 μL). The solution of DNA in an Eppendorf tube sealed with parafilm was warmed at 100 °C for 30 min to induce cleavage at the alkylation sites, allowed to cool to 25 °C, and centrifuged. Formamide dye (0.03% xylene cyanol FF, 0.03% bromophenol blue, 8.7% Na_2EDTA 250 mM) was added (5 μL) to the supernatant. Prior to electrophoresis, the sample was denatured by warming at 100 °C for 5 min, placed in an icebath, and centrifuged, and the supernatant (3 μL) was loaded directly onto the gel. Sanger dideoxynucleotide sequencing reactions were run as standards adjacent to the reaction samples. Polyacrylamide gel electrophoresis (PAGE) was run on an 8% sequencing gel under denaturing conditions (8 M urea) in TBE buffer (100 mM Tris, 100 mM boric acid, 0.2 mM Na_2EDTA) followed by autoradiography.

DNA Alkylation: Relative Rate of (+)-Duocarmycin SA (2), (+)-CBI−TMI, and (+)-MCBI−TMI (40). Following the procedure detailed above, Eppendorf tubes containing 5′ end-labeled w794 DNA (9 μL) in TE buffer (pH 7.5) were treated with (+)-duocarmycin SA (**2**), (+)-CBI−TMI or (+)-MCBI−TMI (**40**) (1 μL, 10^{-6} M in DMSO). The solutions were mixed and incubated at 4 °C for 1, 2, 4, 6, 8, 10, 12, 15, 24, 36 and 48 h, respectively. Subsequent isolation of the alkylated DNA by EtOH precipitation, resuspension in TE buffer (10 μL, pH 7.5), thermolysis (30 min, 100 °C), PAGE, and autoradiography were conducted as detailed above. A relative rate of k(**2**)/k(**40**) for the alkylation at the w794 high-affinity 5′-AATTA site was derived from the slopes of the plots of integrated optical density (IOD) or percent IOD of the high-affinity alkylation site cleavage bands versus time.

DNA Alkylation: Relative Rate of (+)-DSA−Indole$_2$ and (+)-MCBI−Indole$_2$ (42). Following the procedure detailed above, Eppendorf tubes containing 5′ end-labeled w794 (9 μL) in TE buffer (pH 7.5) were treated with (+)-DSA−indole$_2$ or (+)-MCBI−indole$_2$ (**42**) (1 μL, 10^{-6} M in DMSO). The solutions were mixed and incubated at 25 °C for 1, 2, 4, 6, 8, 12, 21 and 24 h, respectively. Subsequent isolation of the alkylated DNA by EtOH precipitation, resuspension in TE buffer (10 μL, pH 7.5), thermolysis (30 min, 100 °C), PAGE, and autoradiography were conducted as detailed above. A relative rate of k(**42**)/k(DSA−indole$_2$) for the alkylation at the w794 high-affinity 5′-AATTA site was derived from the slopes of the plots of integrated optical density (IOD) or percent IOD of the high-affinity alkylation site cleavage bands versus time.

Acknowledgment. We gratefully acknowledge the financial support of the National Institutes of Health (CA 41986) and the award of a NIH postdoctoral fellowship to J.A.M. (CA 62589). We thank Professor Paul A. Kitos for the in vitro cytotoxic evaluations (Table 2) and Weiya Yun and Christine Tarby for conducting additional solvolysis rate studies on **29** and **30**.

Supporting Information Available: ^{1}H NMR of **25**, **26**, **28**−**30**, and **39**−**47** and tables of the in vitro cytotoxic activity summarized in Figure 2 (17 pages). This material is contained in libraries on microfiche, immediately follows this article in the microfilm version of the journal, and can be ordered from the ACS; see any current masthead page for ordering information.

JO952033G